
A TWO-STAGE BAYESIAN SMALL AREA ESTIMATION METHOD FOR PROPORTIONS

A PREPRINT

✉ James Hogg^{1*} Jessica Cameron^{2,4} Susanna Cramb³ Peter Baade^{1,4} Kerrie Mengersen^{1,2}

¹Centre for Data Science, Queensland University of Technology

²School of Mathematical Sciences, Queensland University of Technology

³Australian Centre for Health Services Innovation, School of Public Health and Social Work, Queensland University of Technology

⁴Descriptive Epidemiology, Cancer Council Queensland

ABSTRACT

With the rise in popularity of digital Atlases to communicate spatial variation, there is an increasing need for robust small-area estimates. However, current small-area estimation methods suffer from various modelling problems when data are very sparse or when estimates are required for areas with very small populations. These issues are particularly heightened when modelling proportions. Additionally, recent work has shown significant benefits in modelling at both the individual and area levels. We propose a two-stage Bayesian hierarchical small area estimation model for proportions that can: account for survey design; use both individual-level survey-only covariates and area-level census covariates; reduce direct estimate instability; and generate prevalence estimates for small areas with no survey data. Using a simulation study we show that, compared with existing Bayesian small area estimation methods, our model can provide optimal predictive performance (Bayesian mean relative root mean squared error, mean absolute relative bias and coverage) of proportions under a variety of data conditions, including very sparse and unstable data. To assess the model in practice, we compare modeled estimates of current smoking prevalence for 1,630 small areas in Australia using the 2017-2018 National Health Survey data combined with 2016 census data.

Keywords Bayesian statistics, sample surveys, small area estimation, area level model, individual level model

* james.hogg@hdr.qut.edu.au

1 Introduction

Although the popularity in using digital health Atlases to effectively communicate spatial patterns continues to rise, data for most health outcomes are generally not available for the entire population and therefore researchers must rely on large surveys to generate estimates for small areas. However, this often results in small sample sizes for each small area. A popular remedy is to employ statistical methods for small area estimation (SAE) which use concordance between survey and census data to generate estimates of small area characteristics [1].

Two common frameworks for SAE are direct and model-based estimators. When sample sizes are large, direct estimators which use only sampled individuals can yield estimates with low mean squared error (MSE). However, for smaller regions direct estimators can exhibit very high MSE [2]. Unlike direct estimators, model-based estimators can borrow statistical strength across areas and thus can provide more efficient estimates [3]. Model-based estimators are the pragmatic choice for situations of data sparsity; when area level sample sizes are very small.

Although model-based SAE methods were initially developed for continuous outcomes, proportions of binary or categorical outcomes such as smoking status, are often more useful in health settings [4]. In the past 35 years, model-based SAE for proportions has seen considerable development [4], although several unique methodological challenges arise when the goal is to estimate proportions as opposed to continuous outcomes.

The first difficulty involves the consistency of direct proportion estimates and their sampling variances [5, 6]. Direct proportion estimates for sparse SAE applications can be very unstable, frequently collapsing to zero or one. In this work, we define these sampled areas as *unstable*. As sparsity increases, the likelihood of this instability also dramatically increases. In conjunction with sparsity, instability is exacerbated when the health characteristic is either rare or very common, or when the sample design is very informative. Furthermore, unstable direct estimates give invalid sampling variances, rendering them inapplicable in standard SAE area-level models [7].

The second difficulty is that the bounded nature of proportions violates key distributional assumptions of both the individual level models [8] and area level models [9]. Although these difficulties can be mitigated to some extent by generalised linear models, such as Beta regression [6], or by appropriate transformations [10], there remains some estimation and computational challenges. Even though substantial research has been done to include the sample design in model-based approaches for Gaussian outcomes [2], equivalent methods for proportions has only become a research focus relatively recently [11, 12, 13, 14].

A final methodological challenge is that methods for proportions suffer from stricter data requirements than those for continuous outcomes. For example, individual level logistic models require covariate microdata for the entire population [15, 14], whereas models for continuous outcomes only require covariate summaries [2]. Although some multilevel regression and poststratification (MrP) models [16] relax these requirements, the necessity for concordance between survey and census covariates continues to limit covariate choices to those in the census. This can be a significant limitation because for some outcomes (e.g. chronic disease), survey-only covariates may be more predictive than the demographic and economic factors available in the census [17]. To date, little work has been done to explore the use of survey-only covariates in model-based SAE.

This work is motivated by issues that arise when using SAE in Australia. Australia's population density is highly variable: about 80% of Australians live in east coast cities, and there are huge inland areas that are sparsely populated [18]. It follows that unless a survey has been designed specifically for SAE, sample sizes for small areas can be prohibitively small and remote areas excluded altogether [19, 20]. A review of SAE papers revealed some international studies using area level sample sizes in excess of 25 [13], with most using sample sizes greater than 50 [11, 14]. By contrast, current Australian surveys, such as the 2017-2018 National Health Survey (NHS), have area level sample sizes ranging from 5 to 13 (see Fig. 1). Of course, the extent of this data sparsity renders many areas without survey data, and although model-based methods can be used to estimate proportions for the nonsampled areas, there is a lack of research to determine the best methods for doing so [21, 22].

Data sparsity has historically been remedied by aggregating to a higher administrative level. However, this approach sacrifices resolution. With the growing demand for estimates at a higher resolution and limited funding for larger surveys, new statistical methods must be developed to address the issue of data sparsity.

The aim of this work is to develop small area model-based methods for proportions that can provide superior estimates for sparse survey data. The method will address the above issues by: (1) providing stable direct estimates; (2) accommodating the survey design; (3) making appropriate use of all available data; and (4) providing estimates for nonsampled areas. Our proposed approach, called the two-stage logistic-normal (TSLN) model, has a two-stage structure where stability is gained via an individual level stage 1 prediction model, followed by an area level stage 2 smoothing and imputation model. We take a Bayesian perspective and estimate the model using Markov chain Monte

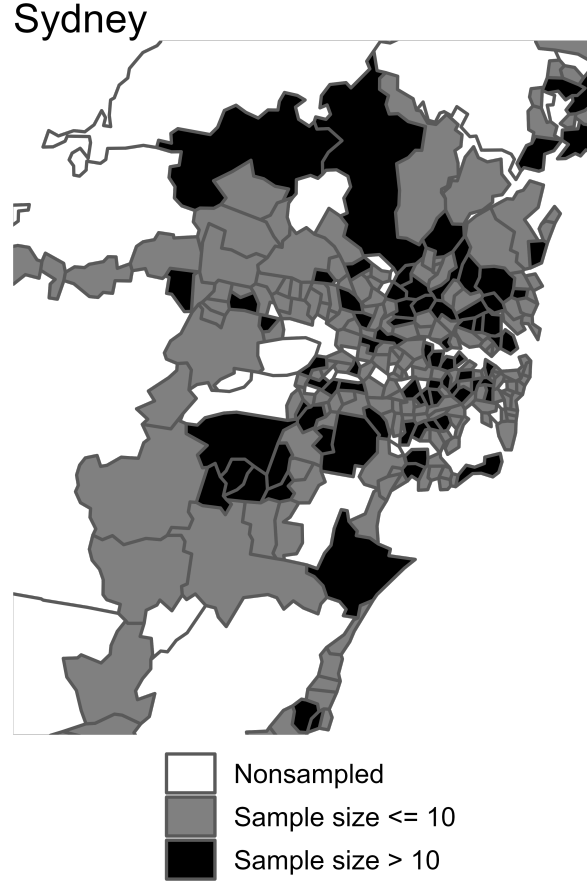


Figure 1: Map of 282 small areas in and around Sydney on the east coast of Australia. Each area is coloured according to the sample size (greater or less than 10) or sample status of the area (sampled or nonsampled) in the 2017-2018 National Health Survey.

Carlo (MCMC) methods [23]. To further contribute to the literature on two-stage approaches we posit two simple metrics to determine the level of smoothing induced by our two-stage approach.

This paper is structured as follows. First, we introduce some notation and describe each stage of our proposed approach. Then we provide details on fitting the TSLN model with Bayesian inference before describing alternative two-stage and one-stage models for proportions. Next, we describe the simulation study conducted to assess the performance of the TSLN model compared with four alternatives. Finally, we provide details on a case study where we generated small area level prevalence estimates of current smoking on the east coast of Australia. In the case study, we demonstrate the flexibility of our approach by including complex random effects and accommodating known benchmarks.

1.1 Notation

We define a finite population, F , with N individuals, where each individual resides in one of M small geographical areas. Allow N_i individuals in each area $i = 1, \dots, M$, such that $\sum_{i=1}^M N_i = N$. We are interested in a binary characteristic $y_{ij} \in \{0, 1\}$ which is equal to 1 if an individual j who resides in area i has the characteristic and 0 otherwise. We wish to generate estimates, $\hat{\mu} = (\hat{\mu}_1, \dots, \hat{\mu}_M)$, of the true proportion of the population with the characteristic, $\mu = (\mu_1, \dots, \mu_M)$.

Without loss of generality, assume that we have samples from the first m areas, $m < M$, and no samples for the remaining $M - m$ areas. Denote the sampled individuals in area i by $j \in r_i$ and the nonsampled individuals by $j \in r_i^C$ where r_i^C is the complement set of r_i . Generally, the survey data used in applications of SAE are collected according to a specified survey design. Design-unbiased population estimates are then derived using the sampling weights, w_{ij}^{raw} , for each sampled individual [2].

Similar to Vandendijck *et al.* [11], we assume that in secondary analysis we do not have sufficient details or data to create weights and instead rely on the weights provided by the data custodians. Note that this is a restrictive assumption as several popular direct estimators require first- and second-order inclusion probabilities for variance estimation [13]. First-order inclusion probabilities give the probability of a person in the sampling frame being in the sample, while second-order inclusion probabilities give the probability of any pair of persons being in the sample. Without sufficient details on the sampling design, second-order inclusion probabilities cannot be calculated.

Throughout this work, $\hat{\mu}_i^D$, $\hat{\mu}_i$, μ_i will denote a direct estimate (using the Hajek [24]), a model-based estimate and the unknown true small area proportion, respectively. Hence,

$$\hat{\mu}_i^D = \frac{\sum_{j \in r_i} w_{ij} y_{ij}}{n_i}. \quad (1)$$

By assuming $w_{ij} = w_{ij}^{\text{raw}} \left(\frac{n_i}{\sum_{j \in r_i} w_{ij}^{\text{raw}}} \right)$ and that all the sampling fractions, $\frac{n_i}{N_i}$, are sufficiently small, we use the following approximation to the sampling variance of the direct proportion estimator [11, 25],

$$\begin{aligned} \psi_i^D = \hat{v}(\hat{\mu}_i^D) &= \frac{1}{n_i} \left(1 - \frac{n_i}{N_i} \right) \left(\frac{1}{n_i - 1} \right) \\ &\quad \sum_{j \in r_i} \left(w_{ij}^2 (y_{ij} - \hat{\mu}_i^D)^2 \right), \end{aligned} \quad (2)$$

which is strictly between 0 and 0.25. Direct estimators have low variance and are design-unbiased for μ_i when n_i is large, but high variance when n_i is small [1]. Although, model-based methods can be biased, they improve variance, resulting in lower MSEs [26].

2 Proposed method

2.1 TSLN model

The proposed two-stage logistic-normal (TSLN) model involves two stages. First an individual level logistic model is fit to the survey data, where individual level predictions are used to generate area estimates [27]. Second, the area estimates are fed into an area level Fay and Herriot [9] (FH) model for further smoothing and to impute proportion estimates for nonsampled areas [13].

2.1.1 Stage 1

The goal of the first stage model is to stabilise the area level direct estimates and sampling variances whilst simultaneously reducing their bias. This is achieved by fitting a Bayesian pseudo-likelihood logistic mixed model to the individual level binary outcomes, y_{ij} . The Horvitz-Thompson estimator of the population-level log likelihood is used to ensure the predictions, p_{ij} , from the logistic model are unbiased under the sample design [28, 12, 14] (see Supplemental Materials B). The first stage model is,

$$\begin{aligned} y_{ij} &\sim \text{Bernoulli}(p_{ij})^{\tilde{w}_{ij}} \\ \text{logit}(p_{ij}) &= \mathbf{x}_{ij}\boldsymbol{\beta} + e_i \\ e_i &\sim N(0, \sigma_e^2) \end{aligned} \quad (3)$$

where $j = 1, \dots, n_i$; $i = 1, \dots, m$. Above, $\mathbf{x} \in \mathbb{R}^{n \times (q^u + 1)}$ is the unit (or individual) level sample design matrix, which includes the q^u fixed effects (individual level survey-only and area level fixed effects), and $\boldsymbol{\beta} \in \mathbb{R}^{(q^u + 1) \times 1}$ the corresponding regression coefficients. Following the notation of Parker, Janicki, and Holan [14], we represent the pseudo-likelihood for a probability density function, $p(\cdot)$, as $p(y_{ij})^{\tilde{w}_{ij}}$, where \tilde{w}_{ij} are the sample scaled weights, $\tilde{w}_{ij} = w_{ij}^{\text{raw}} \left(\frac{n_i}{\sum_{i=1}^m \sum_{j=1}^{n_i} w_{ij}^{\text{raw}}} \right)$. Independent weakly informative priors are placed on the model parameters σ_e , $\boldsymbol{\beta}$. The first-stage model will be referred to as the TSLN-S1 model hereafter.

2.1.2 Stage 1 (S1) estimates

To collapse the individual level data to area level data we calculate S1 proportion estimates, $\hat{\mu}_i^{S1}$, and their corresponding sampling variances, ψ_i^{S1} , by using the posterior distribution for the individual level probabilities, p_{ij} instead of the observed binary outcomes, y_{ij} . This smooths the data at the individual level, which, similar to the work by Gao and Wakefield [29], permits one to view the TSLN-S1 model as a model-based smoothing method. Using S1 estimates guarantees that the values are more stable: all $\hat{\mu}_i^{S1} \in (0, 1)$ and $\psi_i^{S1} \in (0, 0.25)$.

The stage 1 estimates for $i = 1, \dots, m$ are,

$$\hat{\mu}_i^{S1} = \frac{\sum_{j \in r_i} w_{ij} p_{ij}}{n_i} \quad (4)$$

$$\psi_i^{S1} = \hat{v}(\hat{\mu}_i^{S1}) = \hat{v}(\hat{\mu}_i^D) + \hat{v}(\hat{B}_i) \quad (5)$$

$$\hat{B}_i = \frac{\sum_{j \in r_i} w_{ij} (p_{ij} - y_{ij})}{n_i} \quad (6)$$

where \hat{B}_i quantifies the level of smoothing achieved by using the TSLN-S1 model (See Supplemental Materials A for details). The formula used to calculate both $\hat{v}(\cdot)$ terms is given in (2). Note that unlike Roy *et al.* [27] who used the posterior means and standard deviations of $\hat{\mu}_i^{S1}$ for their final results, we found that these were insufficient when sample sizes were very small.

To accommodate the constraints on the S1 estimates in the stage 2 model, we use the common empirical logistic transformation [10, 25],

$$\hat{\theta}_i^{S1} = \text{logit}(\hat{\mu}_i^{S1}) \quad (7)$$

$$\gamma_i^{S1} = \psi_i^{S1} [\hat{\mu}_i^{S1} (1 - \hat{\mu}_i^{S1})]^{-2} \quad (8)$$

where $\hat{\theta}_i^{S1}$ is the log-odds of the stage 1 estimate for area i and γ_i^{S1} the corresponding sampling variance. The logistic transformation permits the use of a Gaussian likelihood in the stage 2 model, which improves computation and avoids the limitations of the Beta distribution (see Supplemental Materials B).

2.1.3 Assessing smoothing properties

Predictions from the TSLN-S1 model should provide acceptable approximations to the observed values, whilst still ensuring a level of generalisability. Severely overfit TSLN-S1 models will yield minimal smoothing and stability gains, while poor fitting models can exhibit very high sampling variances, biased S1 estimates and inaccurate estimates for nonsampled areas. Therefore, the stability gained from smoothing the individual level data must be balanced by ensuring adequate agreement (and comparable variability) of the S1 and direct estimates. To address this we propose two metrics. The smoothing ratio (SR),

$$SR = \frac{\sum_{i=1}^m \left| \frac{\sum_{j \in r_i} w_{ij} (y_{ij} - p_{ij})}{n_i} \right|}{\sum_{i=1}^m \left| \frac{\sum_{j \in r_i} w_{ij} (y_{ij} - \hat{\mu}_i^D)}{n_i} \right|} \quad (9)$$

$$\hat{\mu}^D = \left(\sum_{i=1}^m \sum_{j=1}^{n_i} w_{ij} \right)^{-1} \sum_{i=1}^m \sum_{j=1}^{n_i} w_{ij} y_{ij},$$

indicates the level of smoothing induced by using the TSLN-S1 model, where a small value indicates undersmoothing and a large value indicates oversmoothing. The SR benchmarks the first-stage model predictions with a model considered to provide maximum smoothing (i.e. where $p_{ij} = \hat{\mu}_i^D, \forall i, j$). Small values of the SR are preferred.

The second metric, denoted as the area linear comparison (ALC) in this work, gives the level of agreement between the S1 and direct estimates. The ALC is equal to the regression coefficient when we regress the posterior median of $\hat{\theta}_i^{S1}$ on

$\hat{\theta}_i^D$ with weights $\frac{1}{\psi_i^D}$. The *ALC* assesses the equivalence of the S1 and direct estimates, where a slope of 1 denotes perfect agreement (i.e. no smoothing). By weighting the OLS estimates by $\frac{1}{\psi_i^D}$ we ensure that highly certain direct estimates (or small $\frac{1}{\psi_i^D}$) are given more weight in the OLS. The construction of this metric reflects one of the goals of the TSLN-S1 model; to smooth areas with high uncertainty more than those with low uncertainty. Although there is no theoretical threshold for when the *ALC* measure indicates oversmoothing, $ALC > 0.5$ is a realistic suggestion. Note that other metrics produced by the weighted linear regression (such as the R^2) may also be informative.

2.1.4 Stage 2

By construction, it is reasonable to assume that $\hat{\theta}_i^{\text{S1}}$ follows an approximate Gaussian distribution. Further smoothing of the S1 estimates is achieved by fitting a Bayesian FH model. The second stage model, referred to as the TSLN-S2 model hereafter, is composed of a sampling model,

$$\hat{\theta}_i^{\text{S1}} \sim N(\hat{\theta}_i, \gamma_i^{\text{S1}}), \quad (10)$$

which accommodates the sampling variance of the input data for $i = 1, \dots, m$, and a linking model,

$$\begin{aligned} \hat{\theta}_i &= \mathbf{Z}_i \boldsymbol{\lambda} + v_i \\ v_i &\sim N(0, \sigma_v^2), \end{aligned} \quad (11)$$

which relates the modelled values, $\hat{\theta}_i$, to a series of covariates and area level random effects $\mathbf{v} = (v_1, \dots, v_M)$ for $i = 1, \dots, M$. We use independent weakly informative priors on the model parameters $\sigma_v, \boldsymbol{\lambda}$. The parameter of interest is the posterior distribution of $\hat{\mu}_i = \text{logit}^{-1}(\hat{\theta}_i)$, which can be summarized by deriving summary quantities (such as means, variances and highest density intervals) of the posterior draws of $\hat{\mu}_i$ [30, 1, 2]. Although the specification above is generic, model extensions are, of course, possible. For example, we use the spatial BYM2 prior [31] for v_i in our case study in [Section 5](#).

Note that $\mathbf{Z} \in \mathbb{R}^{M \times (q^a+1)}$ is the area level design matrix, which should include q^a area level covariates that are available for all M areas, and $\boldsymbol{\lambda} \in \mathbb{R}^{(q^a+1) \times 1}$ is the corresponding regression coefficients for the $q^a + 1$ covariates. Although S1 estimates are not available for areas $m+1, \dots, M$, Tzavidis *et al.* [32] show how estimates can be obtained by combining the areas' known covariate values (i.e. \mathbf{Z}) and random draws from the priors.

2.1.5 Generalized variance functions (GVF)

FH models require valid direct estimates and sampling variances for *all* sampled areas. As discussed previously, for very sparse survey data, many sampled areas may give unstable direct estimates ($\hat{\mu}_i^D = 0$ or 1) and thus sampling variances that are undefined or exactly zero.

Although S1 estimates do not suffer from the same instabilities as direct estimates, S1 sampling variances do exhibit undesirable limit properties as they are derived from probabilities rather than binary random variables. For example, consider a single area i with a sample size of 4 and assume that $w_{ij} = 1, \forall j$. While it is possible for $\hat{\mu}_i^{\text{S1}} = 0.01$, to obtain $\hat{\mu}_i^D = 0.01$ one would require 25 times the sample size. In other words, for a fixed sample size S1 estimates are able to be much closer to zero (or one), without being exactly zero (or one), than direct estimates. The result of this phenomenon is unrealistically low S1 sampling variances for unstable areas.

Our solution is to use generalized variance functions (GVF), which relate the sampling variance of a direct estimate to a set of covariates, often including the sample sizes and direct estimates, with necessary transformations [33, 2, 34]. To ensure that S1 sampling variances for unstable areas do not inadvertently affect the fit of the FH model in (10), we impute the $m - m_s$ S1 sampling variances using GVF, where $m_s < m < M$ is the number of stable areas.

In this work, we generalise the approach used by Das *et al.* [35], to a fully Bayesian framework by implementing the following GVF within our model. By fitting the GVF and stage 2 model jointly, such as that by Gao and Wakefield [29], we ensure the uncertainty of the imputations are appropriately taken into account. We use the stable S1 sampling variances to estimate the parameters of the GVF and then use the fitted GVF to impute the S1 sampling variances for the unstable areas.

By letting $f(\cdot)$ be an appropriate link function, \mathbf{L} an area level design matrix, and $\boldsymbol{\omega}$ the corresponding regression coefficients,

$$f(\gamma_i^{S1}) \sim N(\mathbf{L}_i \boldsymbol{\omega}, \sigma_{\text{gvf}}^2), \quad (12)$$

where $i = 1, \dots, m_s$. The S1 sampling variances for $i = m_s + 1, \dots, m$ are imputed by

$$\gamma_i^{S1} = f^{-1}(\mathbf{L}_i \boldsymbol{\omega}). \quad (13)$$

The general form specified in (12) can be adopted according to the scale of the sampling variances and covariates. Note that when $f(x) = \log(x)$, we use the following bias correction used by Das *et al.* [35] when back-transforming, $\gamma_i^{S1} = \exp(\mathbf{L}_i \boldsymbol{\omega} + 0.5\sigma_{\text{gvf}}^2)$. For the TSLN-S2 model, we set $f(x) = \log(\sqrt{x})$ and use $\log(n_i)$ as the single covariate.

2.2 Implementation

While the TSLN model is framed as a single Bayesian model, it is computationally necessary to fit the two stages separately. The TSLN model was fitted using Stan, leveraging its efficient Hamiltonian Monte Carlo (HMC) algorithm [36]. We generated T posterior draws for each parameter in the TSLN-S1 model and then passed (a random subset of) the posterior draws of the relevant parameter estimates as inputs to the TSLN-S2 model. Although we explored more complex approaches to estimating the parameters of the TSLN model, these introduced significant computational and MCMC convergence problems, which may be solved in future work. More details of our inference approach and some alternatives are given in Supplemental Materials A.

3 Existing methods

3.1 Alternative two-stage approaches

Two stage approaches have been used in other SAE methodological work. First and foremost is an approach given by Gao and Wakefield [13], who proposed a smoothed model-assisted small area estimation technique (hereafter named the GW model) by leveraging a logistic generalized regression estimator (LGREG) [38] at the first stage, followed by an area level model to further smooth the stage 1 estimates. Another two-stage approach was implemented by Das *et al.* [35] (hereafter named the DBBH approach), who used cross-sectional FH models to smooth direct estimates before feeding these into multilevel time-series models. In addition, inspiration is drawn from Honaker and Plutzer [39] who considered MrP as a multiple imputation problem and suggested a two-stage approach where the uncertainty induced during individual level modelling could be incorporated into a second stage area level model. Note that both the GW and DBBH approaches support the utility of multi-stage smoothing in SAE which is a key advantage of the TSLN model.

Although our work has similar intuition to both the GW and DBBH approaches, there are several benefits of our model. Firstly, unlike previous approaches which treat predictions from the first stage as fixed, the TSLN-S2 model accommodates the uncertainty in the model parameters and predictions from the TSLN-S1 model. Gao and Wakefield [13] warn against overconfident estimates from their approach as their first stage LGREG estimator is fit using frequentist inference and ignores model parameter uncertainty. By using Bayesian inference at both the individual and area level, our estimates inherit the uncertainty of all model parameters.

Secondly, our approach relaxes some covariate requirements. By relying on the assumption that the first-stage model fit to the survey data is consistent with the true population model, the GW model estimates “unbiased” predictions for all individuals and thus, all areas. This highlights two important data requirements underlying the work by Gao and Wakefield [13]: individual level covariates must be available for all population individuals and survey-only covariates cannot be used. The TSLN model has no such requirement, permitting the use of individual level survey-only covariates. Note that Gao and Wakefield [13] acknowledge the limitations of requiring access to covariate information for the entire population. Their solution was to redefine individuals as very fine spatial grids, where population data were available.

Next, the GW approach requires access to first and second-order inclusion probabilities in order to calculate the sampling variance of their first stage LGREG estimates. In most cases, first-order inclusion probabilities are not provided by data custodians, and further it is very rare to have access to second-order probabilities. Our TSLN model only assumes access to sample weights, which are commonly provided with survey data. Furthermore, unlike the GW model which does not incorporate area level covariates, because of our second stage FH setup, the TSLN model can naturally include area level fixed effects and accommodate the spatially structured and unstructured priors utilized by Gao and Wakefield [13]. Finally, in contrast to the DBBH approach, which operates at the area level only, the TSLN model can provide more efficient estimates by smoothing the data at both the individual and area levels.

Name	Model		Model-based estimate	Limitations	Reference
Pseudo-likelihood logistic model (LOG)	$y_{ij} \sim \text{Bernoulli}(p_{ij})^{\tilde{w}_{ij}}$ $\logit(p_{ij}) = \mathbf{x}_{ij}\boldsymbol{\beta} + e_i$ $j = 1, \dots, n_i; i = 1, \dots, M$	$j = 1, \dots, n_i; i = 1, \dots, m$	$\hat{p}_i = \frac{1}{N_i} \sum_{j=1}^{N_i} p_{ij}$	Requires access to covariate data for the entire population	[12, 14]
Binomial model (BIN)	$\hat{Y}_i = \sum_{j \in r_i} y_{ij}$ $\hat{Y}_i \sim \text{Binomial}(n_i, \hat{\mu}_i)$ $\text{logit}(\hat{\mu}_i) = \mathbf{Z}_i \boldsymbol{\lambda} + v_i$	$i = 1, \dots, m$	$\hat{\mu}_i$	Does not accommodate sample design	[4, 37]
∞ Beta model (BETA)	$\hat{\mu}_i^D \sim \text{Beta}(\kappa_i^{(1)}, \kappa_i^{(2)})$ $\kappa_i^{(1)} = \hat{\mu}_i \phi_i$ $\kappa_i^{(2)} = \phi_i - \kappa_i^{(1)}$ $\phi_i = \frac{\hat{\mu}_i(1 - \hat{\mu}_i)}{\psi_i^D} - 1$ $\text{logit}(\hat{\mu}_i) = \mathbf{Z}_i \boldsymbol{\lambda} + v_i$	$i = 1, \dots, m$	$\hat{\mu}_i$	Requires $\hat{\mu}_i^D \in (0, 1)$ and $\psi_i^D \in (0, 0.25)$, $\forall i$ Possible bimodal posterior Requires GVF for unstable and missing areas Areas with very large ψ_i^D , give μ_i values close to 0.5	[6]
Empirical-logistic normal model (ELN)	$\hat{\theta}_i^D = \text{logit}(\hat{\mu}_i^D)$ $\gamma_i^D = \psi_i^D [\hat{\mu}_i^D (1 - \hat{\mu}_i^D)]^{-2}$ $\hat{\theta}_i^D \sim N(\hat{\theta}_i, \gamma_i^D)$ $\hat{\theta}_i = \mathbf{Z}_i \boldsymbol{\lambda} + v_i$	$i = 1, \dots, m$	$\hat{\mu}_i = \text{logit}^{-1}(\hat{\theta}_i)$	Requires $\hat{\mu}_i^D \in (0, 1)$, $\forall i$ Requires GVF for unstable areas	[10, 25]

Table 1: Description of the individual and area level comparison models with their corresponding model identifiers (e.g. ELN, LOG, etc). Model details can be found in Section 3.2 and Supplemental Materials B, while generalized variance functions (GVFs) are described in Section 2.1.5. Note that $e_i \sim N(0, \sigma_e^2)$ and $v_i \sim N(0, \sigma_v^2)$ and weakly informative priors are generally placed on the parameters, $\boldsymbol{\lambda}, \boldsymbol{\beta}$, σ_e and σ_v . \tilde{w}_{ij} are sampled-scaled weights (see Section 2.1.1) and $\kappa_i^{(1)}, \kappa_i^{(2)}$ are the two parameters of the Beta distribution (see Supplemental Materials B).

Although not discussed in previous work, we found that the quality of the first stage model can play a critical role in the performance of two-stage approaches. Thus, the final benefit of our research is the proposal of a set of metrics (the *SR* and *ALC* in [Section 2.1.2](#)) and recommendations to ensure the two stages complement each other.

3.2 Models for proportions

As with the TSLN model, the GW and DBBH techniques are composed of basic component models such as the logistic and FH. [Table 1](#) gives an overview of four different model-based techniques for small area estimation of proportions that serve as comparison models in the simulation experiment described in [Section 4](#). However, now we briefly address some of the challenges and limitations of these and other alternative methodologies (see Supplemental Materials B for more details), as well as how the TSLN model offers some solutions. In addition, we justify the four comparison models used in this work.

Despite their common use [2], standard FH models may not be suitable for modelling sparse binary data, which can give unstable direct estimates. While unstable sampling variances can be imputed using GVF, some solutions to unstable direct estimates include: small conditional or unconditional perturbations prior to modelling, use of zero-or-one inflated models [40, 41], assuming a distributional form for the strata-specific proportions [10, 42] or dropping them from analysis altogether [6].

BIN model Instability is reduced by considering an aggregation of the binary outcomes via a binomial model. However, these do not generally accommodate the sample design. In contrast, our approach provides stable direct estimates and accommodates the sample design. The binomial model we use in this study purposely ignores the sample design and was chosen as a baseline (crude) model against which the TSLN model was evaluated in terms of sample design consistency.

BETA model Although the Beta distribution is a natural consideration when modelling proportions [43, 5, 6], it has several statistical and computational limitations that are summarized in [Table 1](#) and discussed in detail in Supplemental Materials B. These include: problematic constraints on the $\hat{\mu}_i$'s which depend on the ψ_i^D 's; the necessity to impute sampling variances for non-sampled areas; bimodal behaviour which causes significant MCMC convergence issues; and undefined likelihoods for unstable direct estimates. Nevertheless, the FH Beta model is a popular solution to modelling proportions; thus, it was chosen as one of the comparison models.

ELN model Other area-level models for proportions assume Gaussian distributions for the direct estimators, allowing the use of typical FH models [5]. This method is effective for applications with large area sample sizes. In the situation of sparsity, however, the Gaussian approximation is insufficient. Instead, researchers use the empirical logistic transformation before using a FH model. This is the technique used by Mercer *et al.* [10] and Cassy *et al.* [25], and us. Since the ELN model is most similar to ours, we used it to assess the benefits of using S1 rather than direct estimates as input data.

LOG model Individual level models for binary data offer significant advantages over the area level models discussed above. Most notably, working at the individual level eliminates the need for direct estimates, and allows for greater model flexibility. However, individual level logistic models require covariate data for *all* population units [44, 15]. If all covariates are categorical, multilevel regression with poststratification (MrP) is a favourable solution [45, 46, 44]. However, MrP relies on the process of poststratifying to known population counts which itself creates issues related to covariate choice and data accessibility [16, 17]. The assumption of known individual level covariate data introduces further restrictions on covariate choice due to necessary concordance between survey and census covariates. As mentioned before, covariates collected in a census may be less predictive of health-related outcomes, whilst individual level survey-only covariates may be more useful. The TSLN-S1 model does not predict values for the whole population, hence easing the requirement for survey-census concordance and permitting the inclusion of survey-only covariates.

Standard logistic mixed models (and by extension, MrP) do not accommodate known sample weights and are susceptible to bias under informative sampling. A simple solution is to include the sample weights as covariates, but this requires imputation for nonsampled individuals [11]. Bayesian pseudo-likelihood [28] is an alternative used by Parker, Janicki, and Holan [14] (see Supplemental Materials B). By construction our TSLN model accommodates the sample design at both stages, via pseudo-likelihood in (3) and the weighted estimators in (4). Using the pseudo-likelihood LOG model (a MrP-style) as a comparison model allows us to evaluate the efficacy of employing survey-only covariates and two-stage methods in general.

		α^s	P^L	P^U
50-50	Sc1	0.8		
	Sc2	1.5	0.35	0.65
Rare	Sc3	0.8		
	Sc4	1.5	0.1	0.4
Common	Sc5	0.8		
	Sc6	1.5	0.6	0.9

Table 2: Summary of the six simulation scenarios. Note that α^s mediates the predictive performance of x^s , with lower values resulting in better prediction of the binary outcome, and P^L and P^U give the lower and upper bounds of the true proportions, respectively (see Supplemental Materials C for more details).

		x^s	x^{cs}	k^a
Individual level	TSLN-S1	✓	✓	✓
	LOG		✓	✓
Area level	TSLN-S2			✓
	ELN			✓
	BETA			✓
	BIN			✓

Table 3: Illustrates which of the simulated covariates, described in Section 4, were used in which models in the simulation study. Ticks denote that the model specified in the row used the covariate (shown in the column) as a fixed effect. The estimated regression coefficients and variance terms varied across models, scenarios and repetitions (see Supplemental Materials C).

4 Simulation Study

To evaluate the performance of the TSLN model, we undertook a simulation experiment based on the approach used by Buttice and Highton [47]. First we generated individual level census data for $M = 100$ small areas with populations ranging from 500 and 3000. The simulated census included the binary outcomes, y , two individual-level covariates (one survey-only categorical covariate, x^s with three groups, and one continuous covariate, x^{cs} available in both the census and survey) and a single area level covariate (k^a). Keeping the census, and thus true proportions, fixed, we then drew $D = 100$ unique (repetitions) surveys, fitting the TSLN and four comparison models (Table 1) to each. We used a sampling fraction of 0.4% and only sampled $m = 60$ areas each repetition. Following Hidiroglou and You [34], we devised the sampling method so that individuals with a binary value of 0 were more likely to be sampled and constructed sample weights to reflect this. The median sample size, n , population size, N , and area sample size, n_i was 768, 177071, and 8 respectively. Note that it is relatively rare for simulation experiments in the SAE literature to use such small area level sample sizes; generally $n_i > 50$ [13, 48, 14, 49], which is less relevant in the Australian context. Unstable direct estimates for all comparison models were stabilised via the simple perturbation method; add or subtract a value of 0.001 to any $\hat{\mu}_i^D = 0$ or 1, respectively, prior to modeling. Extensive details of the simulation algorithm can be found in Supplemental Materials C.

Overall, we wished to explore how the TSLN model performed for sparse survey data (e.g. when all n_i are very small). In addition, we wanted to assess performance for varying degrees of prevalence and for the inclusion of more predictive individual level survey-only covariates. These objectives translated to the six simulation scenarios given in Table 2. Note that Sc1, Sc3, and Sc5 ensure that the survey-only covariate is much more predictive of the outcome than the census-available covariate. Given the informative sample design, the rare scenarios (Sc3 and Sc4) will provide a high number of unstable direct estimates (see Table 4).

As described in Section 3 we compared the performance of our novel model to the four model-based SAE methods summarized in Table 1. The TSLN, BETA, LOG and ELN models were fit using `rstan` in R [36]. The BIN model was fit using JAGS via `rjags` [50]. The covariates used in the models are given in Table 3. Only models deemed to have converged were used in the simulation results. Convergence was assessed using \hat{R} [51]. Any analysis for which at least one parameter of interest had $\hat{R} > 1.02$ was discarded. We used 2,000 post-warmup and 6,000 post-burnin draws for each of four chains for the Stan and JAGS models, respectively. R code to run the simulations, with the necessary Stan and JAGS code is available [here](#).

Noninformative and diffuse priors (e.g. $\lambda \propto 1$ and $\sigma_v \propto 1$) are common choices in Bayesian SAE [2, 22]. Recently however, weakly informative priors, which consider the scale of the data, are preferred to these flat priors [52]. All fixed regression parameters in all models were given a $N(0, 2)$ prior, whilst intercept terms were given a student- $t(df = 3, \mu = 0, \sigma = 1)$ prior. Standard deviation parameters in the TSLN-S1, LOG and BIN models were given a

weakly informative $N(0, 1)^+$ prior, while standard deviation parameters in the BETA, ELN and TSLN-S2 models were given a $N(0, 2)^+$ prior. Priors for the GVF were Cauchy $(0, 2)^+$ for the standard deviations and $N(0, 2)$ for the regression coefficients. Note that the GVF of (12) was necessarily adjusted for the Beta model (See Supplemental Materials B for details). All design matrices were mean centered prior to model fitting and the popular QR decomposition was used [53].

The simulation results for the comparison models for Sc1 and Sc2, for example, should be very similar, apart from any simulation noise. This is because the only differences between Sc1 and Sc2 is the increased predictive accuracy of the survey-only covariates, which are *only* included in the TSLN-S1 model (see Table 2). To ensure internal consistency, we refit the comparison models for each of the six scenarios.

Note that we cannot use the GW model as a comparison model as it uses a frequentist approach for the first stage and requires pairwise sampling probabilities for which we assume are inaccessible. Nor can we compare our approach to the DBBH model as it requires temporal data.

4.1 Performance metrics

To compare the models we use Bayesian performance metrics which are calculated separately depending on whether an area was sampled or nonsampled in repetition d . Unlike common frequentist metrics (see Supplemental Materials C), Bayesian metrics use all the appropriate posterior samples during calculation. Thus, they generally favour posteriors with smaller variance, whilst still penalising inaccuracy. While Bayesian coverage is summed over all areas and repetitions, the remaining metrics are calculated independently for each repetition, d . The simulations provide $100 \times T$ posterior draws for each area, model and scenario. Let $\hat{\mu}_{idt}$ be the t th posterior draw for repeat d in area i and μ_i be the true proportion in area i . Also let $\hat{\mu}_{id}^{(L)}$ and $\hat{\mu}_{id}^{(U)}$ denote the lower and upper bounds, respectively, of the posterior 95% highest density interval (HDI) for area i and repeat d .

Absolute relative bias: ARB_{id}

$$\left| \frac{\frac{1}{T} \sum_{t=1}^T (\hat{\mu}_{idt} - \mu_i)}{\mu_i} \right| \quad (14)$$

Mean ARB: MARB_d

$$\frac{1}{M} \sum_{i=1}^M \text{ARB}_{id} \quad (15)$$

Relative root mean square error: RRMSE_{id}

$$\sqrt{\frac{\frac{1}{T} \sum_{t=1}^T (\hat{\mu}_{idt} - \mu_i)^2}{\mu_i}} \quad (16)$$

Mean RRMSE: MRRMSE_d

$$\frac{1}{M} \sum_{i=1}^M \text{RRMSE}_{id} \quad (17)$$

Coverage

$$\frac{1}{MD} \sum_{i=1}^M \sum_{d=1}^D \mathbb{I}(\hat{\mu}_{id}^{(L)} < \mu_i < \hat{\mu}_{id}^{(U)}) \quad (18)$$

The distribution of the 100 MRRMSE_d and MARB_d values are visualized in Fig. 2 and 3, respectively. To summarize these we take the median of each.

4.2 Results

4.2.1 Stage 1 results

Table 4 summarises the simulated data and provides details on the smoothing properties of the TSLN-S1 model. As anticipated with more predictive individual level covariates (e.g. Sc1 versus Sc2), the SR s are lower, and the ALC s are closer to 1. Interestingly, despite the less predictive scenarios having nearly double the noise on average (see Table 2), there are only subtle differences in the ALC and SR . The biggest effect of having more predictive individual level covariates is the significantly smaller increase in sampling variance, at the cost of a lower level of reduction in MAB. As discussed in previous sections, this pattern is expected because the S1 estimates, by design, will collapse to the direct estimates as the TSLN-S1 model begins to “overfit” the survey data.

		Percent of sampled areas unstable (%)	Posterior medians of SR	Posterior medians of ALC	Percent increase in sampling variance (%)	Percent reduction in MAB (%)
50-50	Sc1	3.3 (1.7, 5.0)	0.50 (0.46, 0.54)	0.70 (0.65, 0.74)	55 (27, 91)	25 (22, 29)
	Sc2	3.3 (1.7, 5.0)	0.56 (0.51, 0.60)	0.64 (0.59, 0.68)	72 (40, 106)	32 (28, 35)
Rare	Sc3	25.0 (21.7, 30.0)	0.46 (0.42, 0.51)	0.79 (0.72, 0.83)	78 (36, 140)	24 (19, 28)
	Sc4	25.0 (21.7, 30.0)	0.49 (0.46, 0.54)	0.75 (0.71, 0.81)	100 (52, 161)	27 (22, 32)
Common	Sc5	1.7 (1.7, 3.3)	0.55 (0.51, 0.58)	0.66 (0.62, 0.71)	66 (28, 107)	29 (26, 32)
	Sc6	1.7 (1.7, 3.3)	0.61 (0.57, 0.64)	0.62 (0.56, 0.65)	81 (38, 125)	37 (34, 41)

Table 4: Overview of the simulation and smoothing properties of the TSLN-S1 model (see Supplemental Materials C), including smoothing ratio, SR (9), weighted OLS, ALC (Section 2.1.2), and mean absolute bias (MAB) along with the interquartile bounds in brackets. Column 1 is derived by calculating the percentage of sampled areas with unstable direct estimates for each repetition, before taking the median (and IQ bounds) of these 100 percentages. Column 2 is derived by calculating the posterior median of the SR for each repetition, before taking the median (and IQ bounds) of these 100 values. Column 3 is derived by taking the median (and IQ bounds) of the 100 ALC values. The fourth column is derived by first calculating the median of the area-specific ratios of the stage 1 sampling variances to the direct sampling variances for each repetition, before taking the median (and IQ bounds) of the 100 values (details are given in Supplemental Materials C). Large values indicate large increases in the S1 sampling variances above that of the direct, which is undesirable. The final column is derived by first calculating the ratio between the MABs for the direct and S1 estimates for each repetition, before taking the median (and IQ bounds) of these 100 ratios (details are given in Supplemental Materials C). Large values indicate larger reductions in MAB when using the S1 estimates, which is preferable.

4.2.2 Overall modelling results

Fig. 2 and 3 compare the distribution of MRRMSE and MARB for the models across the 100 repetitions, for the six scenarios and sample status (sampled and nonsampled areas). Table 5 summarises the results shown in the figures by providing the median across the 100 repetitions and also reports the median credible interval sizes and Bayesian coverage.

Accuracy Overall, the TSLN model provides MRRMSE that are between 28% to 40% smaller than those for the next smallest MRRMSE. Across all scenarios and for sampled areas, at least, the TSLN model provides a 20% to 35% smaller MARB than the next smallest MARB; a clear pattern in Fig. 3. However, for nonsampled areas, the TSLN model does not outperform the alternative models, with MARB values ranging from 1% to 43% bigger than the best performing approach (often the LOG model). These findings for the MARB (nonsampled) were expected given the additional smoothing enforced under the TSLN model. That said, the between-simulation variability of the MARB estimates (e.g. the sizes of the boxes in Fig. 3) suggest that the MARB for the TSLN model is at least comparable to the other models for nonsampled areas.

Supplemental Materials C provides frequentist MSE results [42]. Across all scenarios and for sampled areas we found that the TSLN model had MSE values ranging from 40% to 69% smaller than the next smallest. For nonsampled areas, the LOG model had smaller MSE than that of the TSLN model, apart from in the rare scenarios, where the TSLN model outperformed all comparison models.

Uncertainty Similar to Gomez-Rubio *et al.* [54], we found that the credible intervals for all comparison models were too wide for nonsampled areas, but generally too narrow for sampled areas. The TSLN model had, in most cases, coverage closer to the nominal 95% than the comparison models.

By excluding the BIN model due to its excessive bias, our simulation study found that the TSLN model consistently provided the smallest CI widths, with the improvement most notable for nonsampled areas. For sampled areas, posterior credible intervals were consistently between 9% and 33% smaller than that of the other models. For nonsampled areas the CI widths ranged from 43% to 50% smaller. Since the TSLN-S1 model pre-smooths estimates, the TSLN-S2 model has considerably less variance to accommodate than the ELN and BETA models. This manifests itself in a smaller σ_v (see Supplemental Materials C), which results in less posterior variance (i.e. smaller credible intervals). Interestingly when the perturbation applied to unstable direct estimates is less extreme (e.g. setting any $\hat{\mu}_i^D = 0.01$ instead of 0.001), the size of σ_v and thus the uncertainty can be reduced, in some cases even halved (results not shown).

Covariates We found little performance improvements when we used more predictive individual level covariates in the TSLN-S1 model (e.g. comparing Sc1 to Sc2 for example). We found no differences in MRRMSE, CI width or coverage. That said, there were small improvements in MARB when using the more predictive survey-only covariates. For example, for nonsampled areas, the MARB is 2.07 and 2.12 for Sc3 and Sc4, respectively.

		Sampled areas				Nonsampled areas			
		MRRMSE	MARB	CI width	Coverage	MRRMSE	MARB	CI width	Coverage
50-50	BETA	0.35 (2.26)	0.22 (2.14)	0.46	0.81	0.39 (2.37)	0.14 (1.43)	0.61	1.00
	BIN	0.39 (2.50)	0.38 (3.74)	0.18	0.03	0.39 (2.38)	0.38 (3.79)	0.19	0.03
	ELN	0.33 (2.09)	0.19 (1.89)	0.42	0.93	0.37 (2.27)	0.13 (1.33)	0.63	1.00
	LOG	0.25 (1.60)	0.16 (1.56)	0.32	0.91	0.28 (1.68)	0.10 (0.95)	0.47	1.00
	TSLN	0.16 (1.00)	0.10 (1.00)	0.22	0.95	0.17 (1.00)	0.10 (1.00)	0.23	0.96
	BETA	0.35 (2.22)	0.21 (2.01)	0.46	0.82	0.39 (2.33)	0.14 (1.37)	0.61	1.00
Sc2	BIN	0.39 (2.47)	0.38 (3.51)	0.18	0.02	0.39 (2.37)	0.38 (3.60)	0.19	0.02
	ELN	0.32 (2.07)	0.19 (1.76)	0.42	0.93	0.37 (2.23)	0.14 (1.34)	0.62	1.00
	LOG	0.24 (1.56)	0.16 (1.46)	0.32	0.91	0.27 (1.61)	0.10 (0.93)	0.46	1.00
	TSLN	0.16 (1.00)	0.11 (1.00)	0.22	0.95	0.17 (1.00)	0.11 (1.00)	0.23	0.96
	BETA	0.48 (1.46)	0.31 (1.46)	0.22	0.65	0.52 (1.56)	0.23 (1.13)	0.34	0.98
	BIN	0.51 (1.54)	0.48 (2.24)	0.12	0.08	0.50 (1.51)	0.47 (2.27)	0.14	0.09
Sc3	ELN	0.78 (2.38)	0.55 (2.58)	0.40	0.68	1.01 (3.03)	0.21 (1.00)	0.77	1.00
	LOG	0.50 (1.51)	0.34 (1.60)	0.28	0.81	0.54 (1.62)	0.16 (0.78)	0.43	1.00
	TSLN	0.33 (1.00)	0.21 (1.00)	0.19	0.88	0.33 (1.00)	0.21 (1.00)	0.20	0.89
	BETA	0.48 (1.44)	0.31 (1.42)	0.22	0.65	0.52 (1.55)	0.23 (1.08)	0.34	0.98
	BIN	0.51 (1.51)	0.48 (2.17)	0.12	0.08	0.50 (1.49)	0.47 (2.18)	0.14	0.09
	ELN	0.78 (2.34)	0.55 (2.50)	0.40	0.68	1.01 (3.01)	0.21 (0.95)	0.77	1.00
Rare	LOG	0.50 (1.49)	0.34 (1.55)	0.28	0.81	0.54 (1.60)	0.16 (0.74)	0.43	1.00
	TSLN	0.33 (1.00)	0.22 (1.00)	0.19	0.87	0.34 (1.00)	0.22 (1.00)	0.20	0.89
	BETA	0.15 (1.97)	0.08 (1.67)	0.30	0.88	0.18 (2.24)	0.04 (0.84)	0.43	1.00
	BIN	0.25 (3.14)	0.24 (4.85)	0.19	0.05	0.25 (3.05)	0.23 (4.78)	0.21	0.06
	ELN	0.12 (1.52)	0.07 (1.37)	0.26	0.97	0.13 (1.65)	0.05 (1.12)	0.33	1.00
	LOG	0.11 (1.45)	0.06 (1.33)	0.24	0.97	0.12 (1.55)	0.05 (0.98)	0.30	1.00
Sc5	TSLN	0.08 (1.00)	0.05 (1.00)	0.16	0.95	0.08 (1.00)	0.05 (1.00)	0.17	0.96
	BETA	0.17 (2.03)	0.09 (1.77)	0.31	0.88	0.19 (2.33)	0.05 (0.99)	0.46	1.00
	BIN	0.25 (3.04)	0.24 (4.51)	0.19	0.04	0.25 (2.98)	0.24 (4.55)	0.21	0.07
	ELN	0.13 (1.61)	0.08 (1.44)	0.27	0.97	0.14 (1.70)	0.06 (1.24)	0.34	1.00
	LOG	0.12 (1.41)	0.07 (1.29)	0.24	0.97	0.12 (1.52)	0.06 (1.08)	0.31	1.00
	TSLN	0.08 (1.00)	0.05 (1.00)	0.16	0.98	0.08 (1.00)	0.05 (1.00)	0.17	0.99
Common	BETA	0.17 (2.03)	0.09 (1.77)	0.31	0.88	0.19 (2.33)	0.05 (0.99)	0.46	1.00
	BIN	0.25 (3.04)	0.24 (4.51)	0.19	0.04	0.25 (2.98)	0.24 (4.55)	0.21	0.07
	ELN	0.13 (1.61)	0.08 (1.44)	0.27	0.97	0.14 (1.70)	0.06 (1.24)	0.34	1.00
	LOG	0.12 (1.41)	0.07 (1.29)	0.24	0.97	0.12 (1.52)	0.06 (1.08)	0.31	1.00
	TSLN	0.08 (1.00)	0.05 (1.00)	0.16	0.98	0.08 (1.00)	0.05 (1.00)	0.17	0.99

Table 5: Median of MRRMSE_d, MARB_d, width of 95% posterior credible interval (CI width) and coverage across $D = 100$ repetitions. Bold numbers represent the lowest value in each column, scenario and whether the metric is for sampled or nonsampled areas. For coverage, bold numbers denote the value closest to 0.95. Gray numbers in brackets give the ratio of the value to that of the TSLN model.

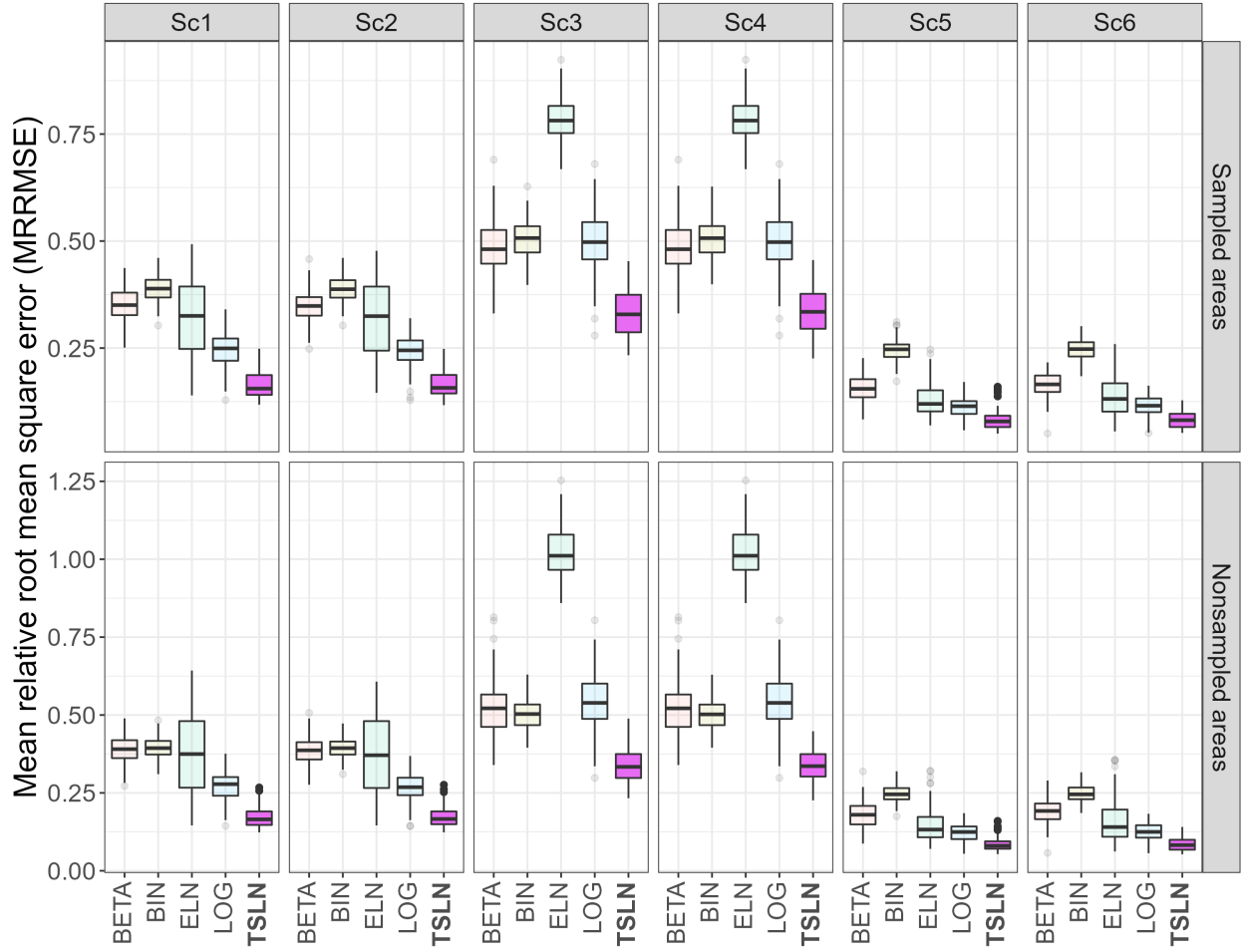


Figure 2: Boxplots of $MRRMSE_d$ across all $D = 100$ repetitions. The medians of each boxplot are available in [Table 5](#).

Rare outcomes Given our interest in small area estimation applications under heavy instability, the simulation results for the rare scenarios (Sc3 and Sc4) are particularly important. Although the ELN and TSLN models are relatively similar in construction, our approach gave superior results under heavy instability. TSLN model had lower median $MRRMSE$, smaller average CI widths, and better coverage than the ELN model. We believe this is primarily due to the substantially larger random effect variance (see Supplemental Materials C); in Sc3 $\sigma_v = 2.14, 0.17$ for the ELN and TSLN models, respectively. Although the alternative area level model, the BETA model, provided better coverage (97%) for non-sampled areas, it gave very poor coverage (67%) for sampled areas. Although individual level models like the LOG model should provide optimal prediction in the unstable setting, we found that the TSLN model remained superior to the LOG model in terms of median $MRRMSE$, average CI width and coverage. For the rare scenarios and for nonsampled areas, the LOG model gave the lowest bias; approximately 41% smaller than the TSLN model. However, the between-simulation variability of the MARB (see [Fig. 3](#)) suggests this difference is not significant.

5 Application: Prevalence of current smoking on the east coast of Australia

To illustrate the benefits of the two-stage logistic normal (TSLN) model in practice, we generate small area estimates of current smoking prevalence in Australia using the TSLN, ELN and LOG models. Neither the BIN model (poor performance in the simulation study) nor the BETA model (has various limitations, see Supplemental Materials B) were considered. Unless otherwise stated, the model specifications used in this application are identical to those described in the preceding sections.

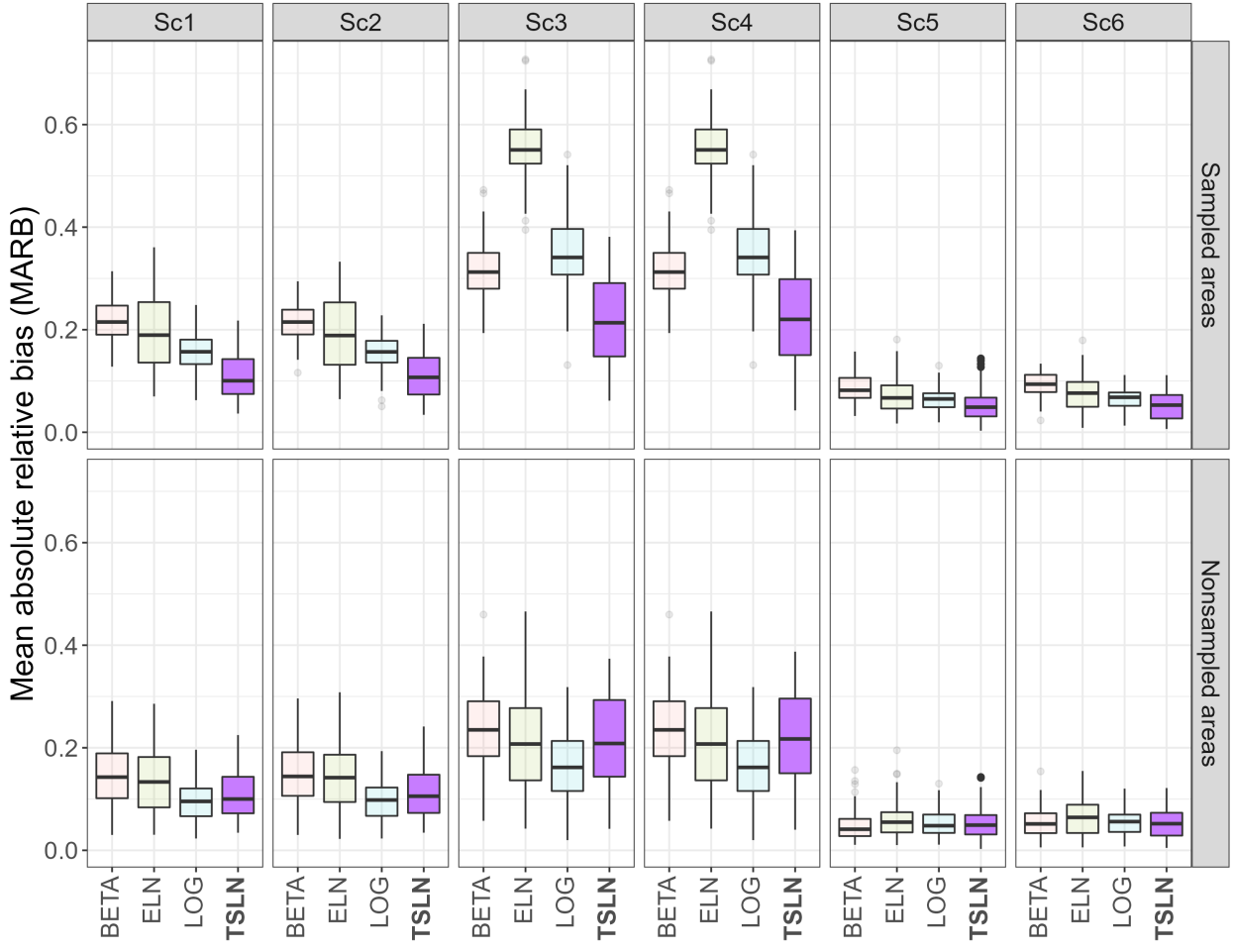


Figure 3: Boxplots of $MARB_d$ across all $D = 100$ repetitions. The medians of each boxplot are available in [Table 5](#). We have omitted the BIN model; its very large bias distorts the plot.

5.1 Data

The individual level survey data were obtained from the 2017-18 National Health Survey (NHS), which is an Australia-wide population-level health survey conducted every 3-4 years by the Australian Bureau of Statistics (ABS) [\[55, 56\]](#). The survey aimed to collect a variety of health data on one adult and one child (where possible) in each selected household. Households were selected using a complex multistage design [\[55\]](#). Trained ABS interviewers conducted personal interviews with selected persons in each of the sampled households. To allow researchers to accommodate the complex sample design, the ABS provides survey weights, which we use in this analysis after applying the necessary rescalings (see [Section 1.1](#)). For the area level auxiliary data, we use data from the 2016 Australian census, represented as proportions. We obtained the Estimated Resident Population (ERP) stratified by age (15 years and above), sex and small area for both 2017 and 2018. In this study the population counts were derived by averaging across the two years. Although the 2017-18 NHS collected data across Australia, we reduce our analysis to just those states on the east coast, both to ease the interpretation of visualizations and reduce the computation time.

We classify current smoking as daily, weekly, or less-than-weekly smokers, like the Social Health Atlas [\[19\]](#). We additionally enforce that all current smokers must have smoked at least 100 cigarettes in their lifetime. After exclusions, we have data for 10,918 respondents aged 15 years and above. The overall weighted prevalence of current smoking in our study region is 14.7%.

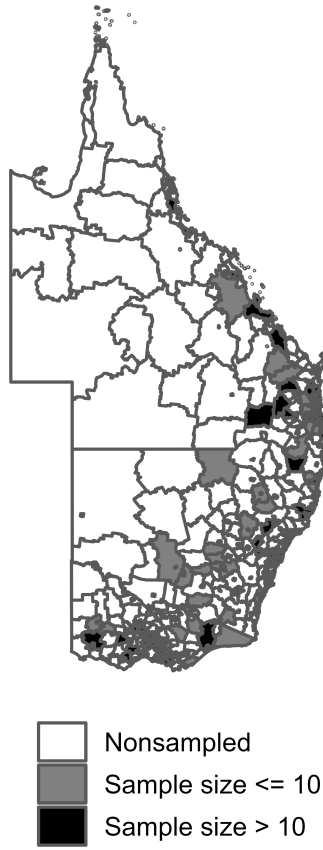


Figure 4: Map of the 1630 statistical area level 2 (SA2s) on the east coast of Australia. Each SA2 is coloured according to the sample size (greater or less than 10) or sample status of the SA2 (sampled or nonsampled).

The goal of this analysis is to generate prevalence estimates for 1,630 small areas, of which 1,262 (77%) were sampled. Of the sampled areas, 781 (62%) gave stable direct estimates. Area level sample sizes range from 1 to 140, with a median of 7. Given that around 50% of the small areas are either missing or unstable (see Fig. 4), it is clear how this SAE application illustrates the sparsity issues we've addressed in this work.

The small areas we use are derived from the 2016 Australia Statistical Geography Standard (ASGS), which is the geographic standard maintained by the ABS [57]. The ASGS splits Australia into a hierarchical structure of areas that completely cover the country. We generate prevalence estimates at the statistical areas level 2 (SA2), which is the lowest level of the ASGS hierarchy for which detailed census population characteristics are publicly available.

5.2 Model details

Model selection is an intricate step of our approach in practice. Not only do we have two models for which variable selection must be performed, but variable selection decisions made at the second stage are dependent on the model fit of the first stage; an issue we do not tackle here. To reduce the computational burden of variable selection, we follow the advice by Goldstein [58] and initially use frequentist AIC, BIC and the *SR* and *ALC* (where applicable) to select fixed effects. Final covariate and random effect decisions were made using Bayesian leave-one-out cross-validation (LOOCV) via Pareto-importance sampling [59]. Lower values of AIC and BIC are preferred, while higher values of LOOCV are preferred. Where possible the fixed and random effects for all the models were chosen according to the TSLN model. That is, to enable fair comparisons, fixed and random effects for all models were as similar as possible. See Supplemental Materials B for further details.

5.2.1 Individual level models

We used the following individual level categorical covariates in the TSLN-S1 model: age, sex and their interaction; registered marital status; high school completion status; Kessler psychological distress score; educational qualifications;

self-assessed health; and labor force status. We also used the following household level categorical covariates: number of daily smokers, tenure type, and whether there were Indigenous Australian household members. Along with the individual and household level covariates, we used some SA2-level contextual covariates including state, the Index of Relative Socio-Economic Disadvantage (IRSD) from the Socio-Economic Indexes for Areas (SEIFA) [60], and the following SA2-level demographic variables as proportions: occupation, Indigenous Australian status, income, unemployment and household composition.

In addition to the individual and area level fixed effects, we added two further random effects. Borrowing ideas from MrP [61], we added a hierarchical prior on a risk factor categorical covariate to the TSLN-S1 model. This risk factor categorical covariate was constructed from every unique combination of sex and age and four binary-coded individual level risk factors resulting in 274 categories. The number of participants in each category ranged from 1 to 299, with a median of 20. Finally, to further improve the predictive accuracy of the TSLN-S1 model and reduce the SR , we also included an individual level residual error term with a fixed standard deviation of 0.5. The chosen TSLN-S1 model had $SR = 0.59$, $ALC = 0.67$.

Since census microdata was unavailable, we could not mirror the TSLN-S1 model complexity in the LOG model. We omitted the risk factor categorical random effect and were restricted to just three individual level covariates: age, sex and marital status. These three covariates gave a poststrata dataset with 146,700 rows. Note that we also omitted the individual level residual error term from the LOG model as, unlike the TSLN-S1 model, the LOG model must prioritise generalisability in order to perform well.

Further details and definitions for the covariates used in the individual level models can be found in Supplemental Materials B.

5.2.2 Area level models

For both the TSLN-S2 and ELN models, we utilized the following SA2-level covariates: IRSD, state and the first six principal components derived from SA2-level census proportion data. Similar to Section 2.1.5 we use GVF_s where the log of the SA2-level sample sizes were the only predictor. Details on variable selection and the covariates used in the area level models can be found in Supplemental Materials D.

5.2.3 Spatial random effects

Unlike in the simulation study where data were not generated with any spatial autocorrelation, we expect smoking prevalence to exhibit spatial clustering as smoking is generally higher in areas of lower socioeconomic status which can be geographical neighbors [62]. It has been shown that accommodating spatial structure in model-based SAE methods can provide considerable efficiency gains [63, 11, 64, 13, 7]. To adjust for the spatial autocorrelation between areas and enforce global *and* local smoothing, we use the BYM2 prior [31] at the SA2-level for the TSLN-S2, ELN and LOG models (see Supplemental Materials D for details). Although others have used conditional autoregressive (CAR) or simultaneous autoregressive (SAR) priors only, Gomez-Rubio *et al.* [54] conclude that models with just the CAR prior generally over-estimate the small area estimates and argue that including a structured and unstructured random effect provides a useful compromise between producing accurate small area estimates and their corresponding variances.

5.2.4 Priors and computation

Most of the priors used in this case study mirror those specified in Section 4. We utilised a relatively informative prior for ρ , the mixing parameter of the BYM2 spatial prior which controls the amount of spatially structured as opposed to unstructured variation, where $\rho = 1$ gives a scaled intrinsic CAR prior [31]. We use $\rho \sim \text{Beta}(\text{shape} = 3.05, \text{rate} = 1.65)$, a prior which places roughly 45% of density above $\rho = 0.7$. In this application, areas with survey data may have many neighbors but few with survey data, thus this informative prior “encouraged” the models to borrow information locally. The median number of neighbors is 7, whereas the median number that have sampled data is 5. This informative prior on ρ slightly improved both model fit and predictive accuracy. The posterior median of ρ was 0.89 under this informative prior, but 0.5 under a Uniform(0, 1) prior.

We used 5000 post-warmup draws for each of four chains in Stan [36], feeding a random subset of 500 posterior draws from the TSLN-S1 to the TSLN-S2 model. For storage reasons we thinned the draws by four, resulting in 5000 useable posterior draws. Convergence of the models were assessed using \hat{R} [51], where a $\hat{R} < 1.02$ was used as the cutoff for convergence for the parameters of interest, namely μ . We also explored trace plots and autocorrelation plots to verify convergence. All proportion parameters, μ , had effective sample sizes > 500 .

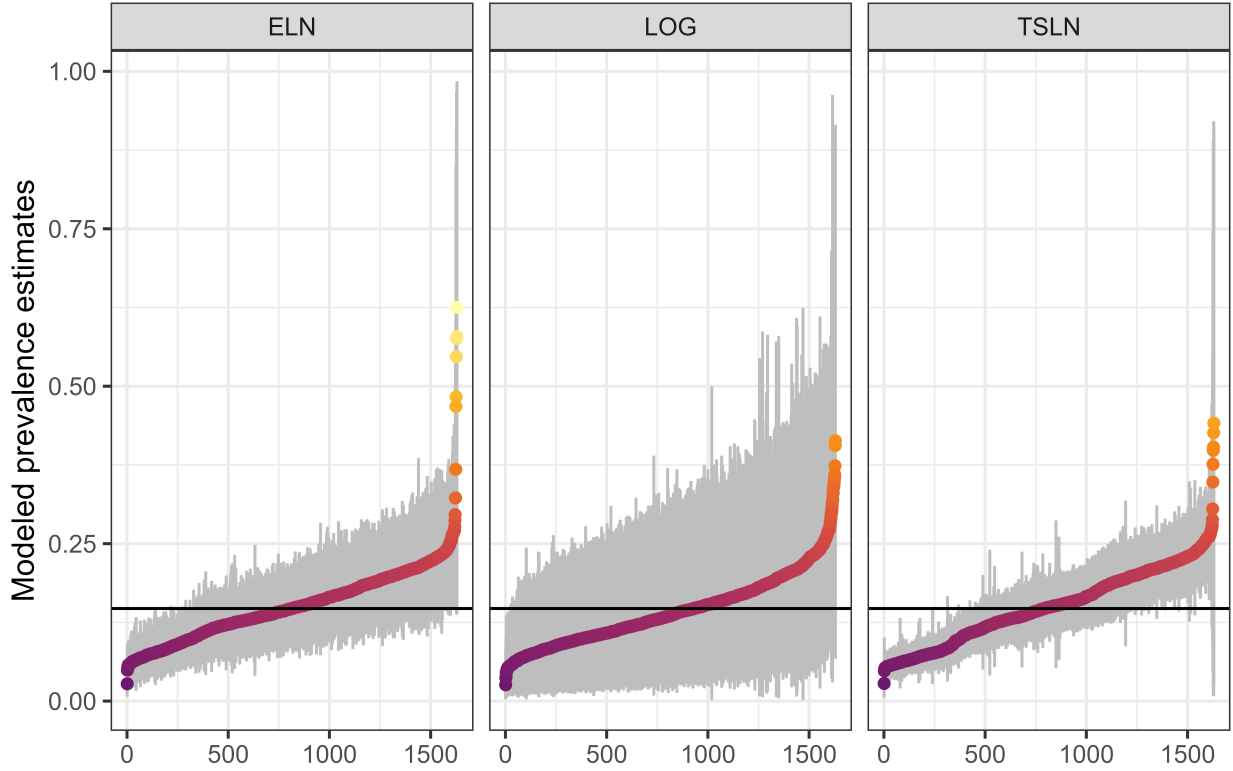


Figure 5: Comparison of the modeled SA2 level current smoking prevalence estimates from the three models. The caterpillar plots displays the posterior medians and 95% highest density intervals (grey bars) for all 1630 SA2s, ordered by their magnitude. The point colors mirror the y -axis and the vertical black line is the overall current smoking prevalence.

5.2.5 Benchmarking

To help validate our small area estimates, we utilised state-level estimates as internal benchmarks [65]. There are four states on the east coast of Australia, with a median sample and population size of 3100 and 4.6 million, respectively. At this level of aggregation, the direct estimates are reliable. We employed inexact fully Bayesian benchmarking [66], which acts as a soft constraint on the model by penalizing discrepancies between the modeled state estimates and the direct state estimates. Unlike previous approaches that use posterior point estimates [1], Bayesian benchmarking directly includes the benchmarks in the joint posterior distribution, which accounts for benchmarking-induced uncertainty. We use Bayesian benchmarking in the TSLN-S2 and ELN models and exact benchmarking for the LOG model. Full details and a performance comparison with and without benchmarking is given in Supplemental Materials D.

5.2.6 Visualisations

We map both absolute and relative measures of current smoking. The absolute measures are the posterior medians and highest density intervals (HDIs) of the estimated prevalence from the models, while the relative measures rely on odds ratios (ORs). We derive ORs as follows,

$$\widehat{OR}_i = \frac{\hat{\mu}_i / (1 - \hat{\mu}_i)}{\hat{\mu}^D / (1 - \hat{\mu}^D)}, \quad (19)$$

where $\hat{\mu}^D$ is the overall direct estimate of current smoking prevalence. By deriving \widehat{OR}_i for all posterior draws, we can map their posterior medians and HDIs. To quantify whether an OR is significantly different to 1, we use the exceedence probability (EP) [67, 37], where $t = 1, \dots, T$ indexes the MCMC draws.

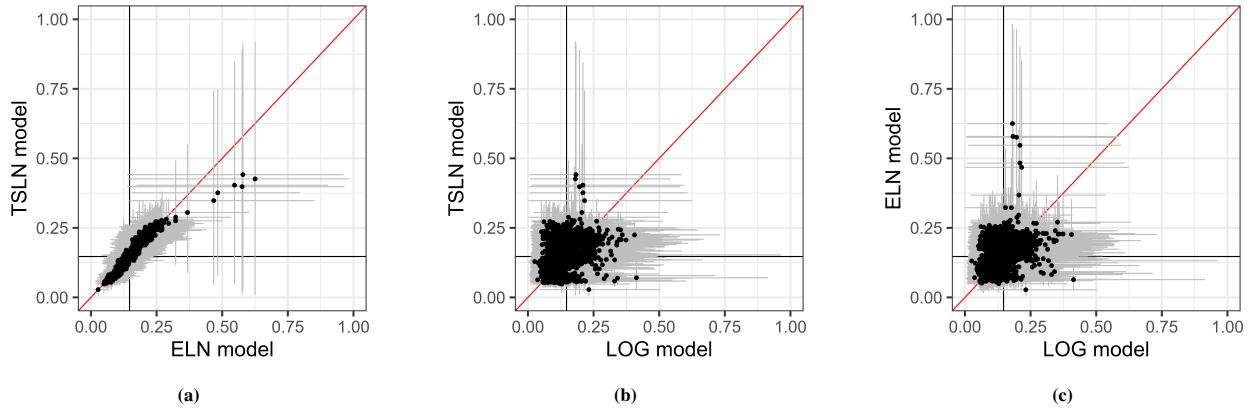


Figure 6: Comparison of the modeled estimates from the TSLN, LOG and ELN models. The scatter plots display the posterior medians (black points) and 95% highest density intervals (gray bars) of the modeled SA2 level current smoking prevalence estimates, with the red lines denoting equivalence. The vertical and horizontal black lines are the overall current smoking prevalence.

$$EP_i = \left(\frac{1}{T} \sum_t \mathbb{I}(\widehat{\text{OR}}_{it} > 1) \right) \quad (20)$$

A high (low) EP_i is interpreted as a high level of evidence that the OR for SA2 i is significantly higher (lower) than 1. Generally an EP_i above 0.8 or below 0.2 is considered significant [68].

5.3 Results

Fig. 5 gives separate caterpillar plots for the SA2-level prevalence estimates and HDIs for the three models. Supporting this plot, **Fig. 6** compares the estimates from the TSLN model to the ELN and LOG models. Both figures show the similarities in the modeled estimates from the two area level models and the superior interval sizes of the TSLN model. The LOG model provides estimates with little correspondence to those from the TSLN or the ELN models.

For areas with high prevalence the TSLN model provides more conservative estimates than those from the ELN model; a result of the two stages of smoothing applied when using the TSLN model. Given that the sparsity of the survey data results in very noisy and unstable direct estimates, in this case study we prefer estimates that are slightly oversmoothed than undersmoothed.

The six outlying points visible in (a) of Fig. 6 are SA2s in the Cape York (Northern section) region of Queensland. The high level of uncertainty for these SA2s is reasonable as they are remote, have small populations and are far from areas with survey data.

In Fig. 7 we map the relative measures for all 1630 SA2s, including those without survey data. The figure displays posterior median ORs, HDIs and corresponding *EPs* for the three models. Observe that because the area level models (TSLN and ELN) generally provide more certainty in the estimates, the *EPs* are more extreme than those for the LOG model. The prevalence of current smoking is significantly higher than the overall prevalence in the west and northern parts of the region, while significantly lower in urban centres, such as Sydney (the most populous city on the east coast of Australia), Melbourne and Brisbane. Fig. 8 gives the absolute prevalence estimates for these three cities. See Supplemental Materials D for a plot stratifying the modeled estimates by socioeconomic status and maps of the absolute prevalence estimates from the models.

By treating the direct estimates at a higher aggregation level as the truth, we compare the direct and modelled estimates at the statistical area level 4 using RRMSE, ARB, coverage and interval overlap. The details and possible limitations of these comparative performance results are given in Supplemental Materials D. We found that the TSLN model provided superior MRRMSE and interval overlap. Furthermore, the performance metrics for the TSLN model show the smallest changes when we benchmark, providing more support for the validity of the TSLN model estimates. Prevalence estimates from the LOG model, on the other hand, saw considerable changes when benchmarking was applied. We posit that the LOG model is providing poor estimates given the restricted set of individual level census covariates that were available, given the requirements of the LOG model.

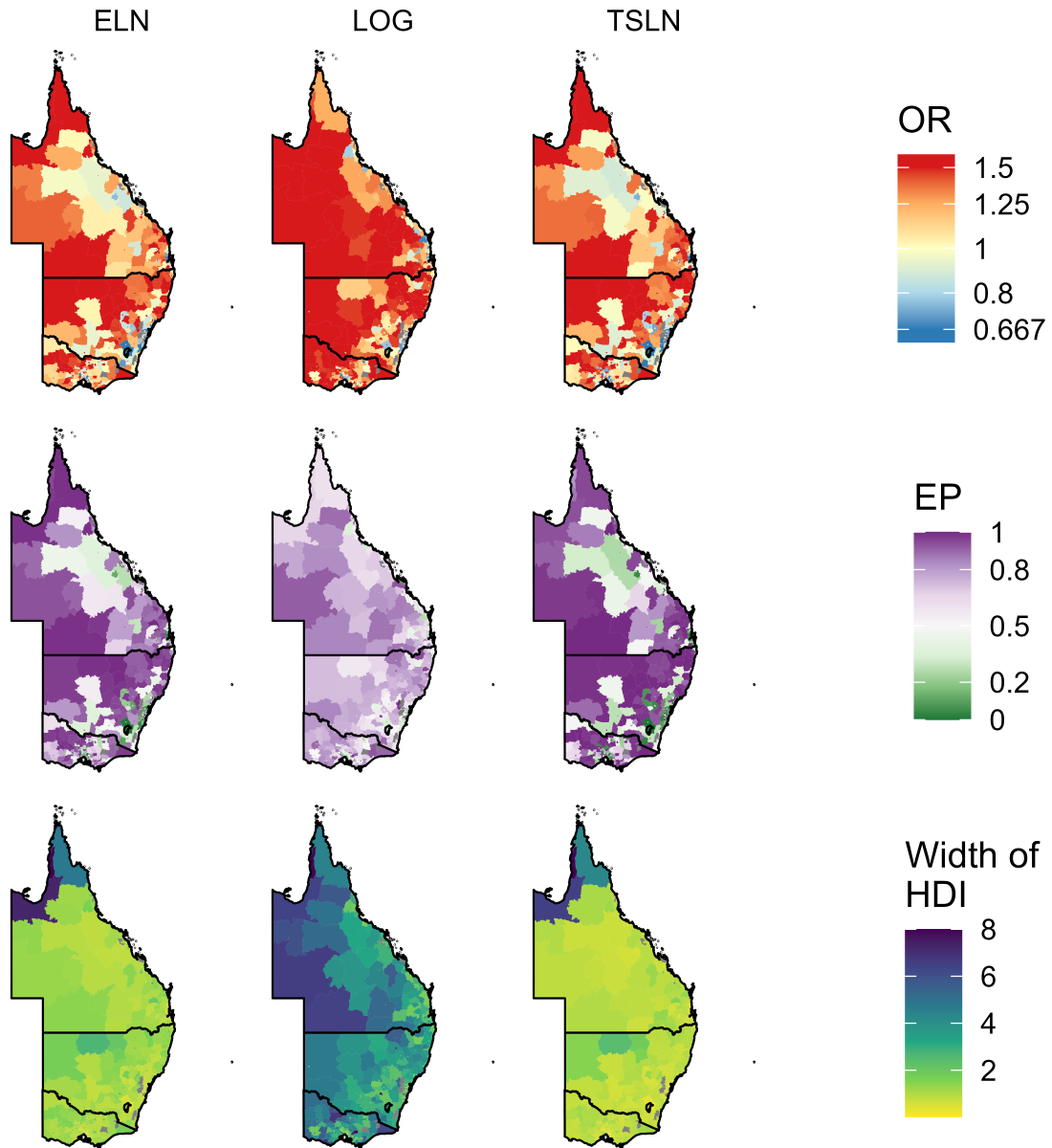
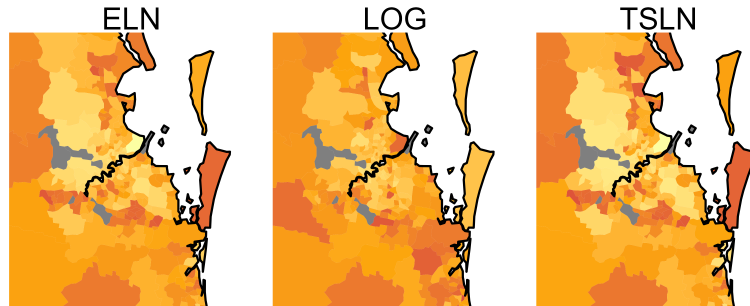
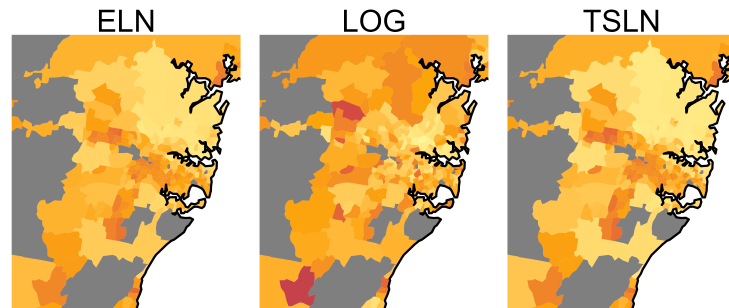


Figure 7: Choropleth maps displaying the modeled ORs for smoking prevalence in 1630 SA2s on the east coast of Australia. For each model, this figure displays the posterior medians (top row), exceedence probabilities (EPs) (middle row) and width of the 95% HDI (bottom row) for the ORs. Note that some values are lower than the range of color scales shown — for these values, the lowest color is shown. Gray areas were excluded from estimation due to having 2016-2017 ERPs smaller than or equal to 10. Black lines represent the boundaries of the four states on the east coast of Australia.

Brisbane



Sydney



Melbourne

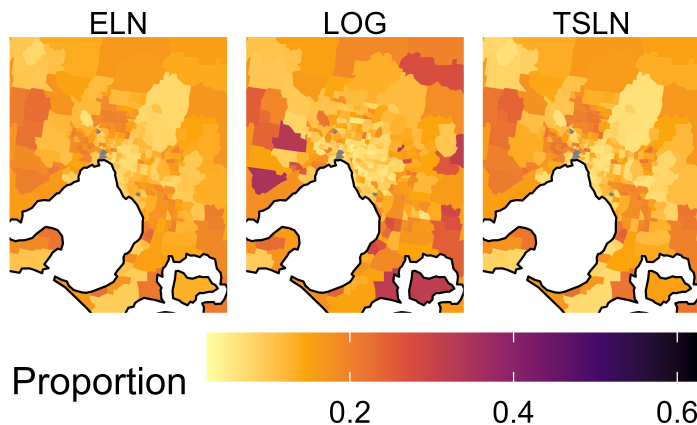


Figure 8: Choropleth inset maps displaying the modeled estimates of the proportion of current smokers in and around Sydney, Melbourne and Brisbane; three capital cities on the east coast of Australia. Gray areas were excluded from estimation due to having 2016-2017 ERPs smaller than or equal to 10. Most of these excluded areas are National parks, industrial areas, airports or cemeteries.

6 Discussion

We have proposed a new method using a Bayesian two-stage model to estimate proportions for small areas from sparse survey data. The TSLN model is able to model these data by reducing instability, accommodating survey design, relaxing restrictions on the covariates that can be included and generating estimates for nonsampled areas. We've shown that the TSLN model can provide superior proportion estimates for sampled and nonsampled areas compared to some alternatives, with similar or slightly more bias but much smaller variance; resulting in consistently smaller MRRMSEs and credible intervals. Compared with other available approaches, the TSLN model appears to be the best option in sparse settings, such as when using the NHS.

We have demonstrated, along with others [13, 35], that the smoothing properties of modelling at both the individual and area level are beneficial across a broad range of SAE applications. That said, although it has not been explicitly acknowledged in earlier research on two-stage approaches, we found that the quality of the first stage model can have a significant impact on the performance of two-stage methods. Thus, in addition to the modeling approach, we have contributed more widely to the two-stage literature by proposing simple measures (e.g., the *SR* and the *ALC*) and recommendations to aid practitioners to ensure that the two-stages work with, rather than against, one another.

Although the simulation results and case study illustrate the potential benefits of the TSLN model, some limitations motivate future theoretical and applied research in two-stage SAE. First, there would be benefits in the development of rigorous statistical theory to motivate the use of S1 estimates over direct estimates. Moreover, there is opportunity for theoretical determination of optimal values for the *SR* and *ALC* in particular two-stage SAE applications. Another avenue of research is the development or application of model-specific MCMC algorithms capable of fitting the TSLN model in one single step. Alternatively, the TSLN model could be redefined using ideas from modular models that leverage Bayesian cut distributions [69]. There is also scope to develop non-GVF solutions to the undesirable properties mentioned in Section 2.1.5 and more formally compare methods to adjust for instability. Although coverage was relatively stable for the TSLN model, one could explore methods of conformal prediction [70], which can be used to guarantee frequentist coverage in small area estimation [71].

The TSLN model is generic in its component models, which within an applied context allows researchers to extend the TSLN model by using more flexible classes of models (such as semi or non-parametric models or even machine learning algorithms), as long as uncertainty can be captured. Moreover, further work is required in developing model selection tools for both stages of the TSLN model, with a focus on the flow-on effect of variable choices in the first stage to the second.

7 Conclusion

Given that the need for higher resolution area level estimates is increasing faster than funding for larger surveys, methods of small area estimation must be capable of tackling sparsity issues. In this work, we have developed a solution to small area estimation for severely sparse data by leveraging both area and individual level models and utilising more auxiliary data (namely, survey-only covariates). Similar to other work [13, 35], this research represents another important step in continuing the positive narrative surrounding two-stage approaches and highlights their benefits and future avenues of research in small area estimation. As expressed by Fuglstad, Li, and Wakefield [4], “... the goal of the analysis should determine the approach, and different goals may call for different approaches.” We hope our approach will afford practitioners to set more ambitious goals for their small area estimates; lower levels of aggregation or deriving estimates by area *and* sex or age.

Acknowledgments

This study has received ethical approval from the Queensland University of Technology Human Research Ethics Committee (Project ID: 4609) for the project entitled “Statistical methods for small area estimation of cancer risk factors and their associations with cancer incidence”.

We thank the Australian Bureau of Statistics (ABS) for designing and collecting the National Health Survey data and making it available for analysis in the DataLab. The views expressed in this paper are those of the authors and do not necessarily reflect the policy of QUT, CCQ or the ABS.

Competing interests

The authors declare that they have no competing interests.

Funding

JH was supported by the Queensland University of Technology (QUT) Centre for Data Science and Cancer Council QLD (CCQ) Scholarship. SC receives salary and research support from a National Health and Medical Research Council Investigator Grant (#2008313).

Supplemental materials

The supplemental material mentioned throughout this work can be found on at the end of this document. This additional material includes further details, plots and results to accompany Sections 2-5 of this paper.

References

- [1] Danny Pfeffermann. New important developments in small area estimation. *Statistical Science*, 28(1):40–68, 2013.
- [2] J.N.K. Rao and Isabel Molina. *Small Area Estimation*. Wiley Series in Survey Methodology, Hoboken, New Jersey, 2nd edition, 2015.
- [3] A. Moretti and A. Whitworth. Estimating the uncertainty of a small area estimator based on a microsimulation approach. *Sociological Methods and Research*, 2021. doi:[10.1177/0049124120986199](https://doi.org/10.1177/0049124120986199).
- [4] Geir-Arne Fuglstad, Zehang Richard Li, and Jon Wakefield. The two cultures for prevalence mapping: Small area estimation and spatial statistics. *arXiv preprint arXiv:2110.09576*, 2021. doi:[arXiv:2110.09576](https://arxiv.org/abs/2110.09576).
- [5] Benmei Liu, Partha Lahiri, and Graham Kalton. Hierarchical bayes modeling of survey-weighted small area proportions. *Proceedings of the American Statistical Association, Survey Research Section*, pages 3181–3186, 2007.
- [6] R. Janicki. Properties of the beta regression model for small area estimation of proportions and application to estimation of poverty rates. *Communications in Statistics - Theory and Methods*, 49(9):2264–2284, 2020. doi:[10.1080/03610926.2019.1570266](https://doi.org/10.1080/03610926.2019.1570266).
- [7] John Paige, Geir-Arne Fuglstad, Andrea Riebler, and Jon Wakefield. Design-and model-based approaches to small-area estimation in a low-and middle-income country context: comparisons and recommendations. *Journal of Survey Statistics and Methodology*, 10(1):50–80, 2022. ISSN 2325-0984.
- [8] George E. Battese, Rachel M. Harter, and Wayne A. Fuller. An error-components model for prediction of county crop areas using survey and satellite data. *Journal of the American Statistical Association*, 83(401):28–36, 1988. ISSN 0162-1459. doi:[10.1080/01621459.1988.10478561](https://doi.org/10.1080/01621459.1988.10478561).
- [9] Robert E. Fay and Roger A. Herriot. Estimates of income for small places: An application of james-stein procedures to census data. *Journal of the American Statistical Association*, 74(366):269–277, 1979. ISSN 01621459. doi:[10.2307/2286322](https://doi.org/10.2307/2286322).
- [10] Laina Mercer, Jon Wakefield, Cici Chen, and Thomas Lumley. A comparison of spatial smoothing methods for small area estimation with sampling weights. *Spatial Statistics*, 8(1):69–85, 2014. ISSN 2211-6753. doi:<https://doi.org/10.1016/j.spasta.2013.12.001>.
- [11] Y. Vandendijck, C. Faes, R. S. Kirby, A. Lawson, and N. Hens. Model-based inference for small area estimation with sampling weights. *Spatial Statistics*, 18(1):455–473, 2016. doi:[10.1016/j.spasta.2016.09.004](https://doi.org/10.1016/j.spasta.2016.09.004).
- [12] Terrance D Savitsky and Daniell Toth. Bayesian estimation under informative sampling. *Electronic Journal of Statistics*, 10(1):1677–1708, 2016. ISSN 1935-7524.
- [13] Peter A. Gao and Jonathan Wakefield. Smoothed model-assisted small area estimation. *arXiv preprint arXiv:2201.08775*, 2022. doi:[arXiv:2201.08775](https://arxiv.org/abs/2201.08775).
- [14] Paul A. Parker, Ryan Janicki, and Scott H. Holan. Unit level modeling of survey data for small area estimation under informative sampling: A comprehensive overview with extensions. *arXiv preprint arXiv:1908.10488*, 2019. doi:[arXiv:1908.10488](https://arxiv.org/abs/1908.10488).
- [15] F. A. S. Moura and H. S. Migon. Bayesian spatial models for small area estimation of proportions. *Statistical Modeling*, 2(3):183–201, 2002. doi:[10.1191/1471082x02st032oa](https://doi.org/10.1191/1471082x02st032oa).
- [16] Lucas Leemann and Fabio Wasserfallen. Extending the use and prediction precision of subnational public opinion estimation. *American Journal of Political Science*, 61(4):1003–1022, 2017. ISSN 0092-5853. doi:<https://doi.org/10.1111/ajps.12319>.

[17] Shiro Kuriwaki and Soichiro Yamauchi. Synthetic area weighting for measuring public opinion in small areas. *arXiv preprint arXiv:2105.05829*, 2021. doi:[arXiv:2105.05829](https://arxiv.org/abs/2105.05829).

[18] B. Baffour, H. Chandra, and A. Martinez. Localised estimates of dynamics of multi-dimensional disadvantage: An application of the small area estimation technique using australian survey and census data. *International Statistical Review*, 87(1):1–23, 2019.

[19] PHIDU. Social health atlases, 2018. <https://phidu.torrens.edu.au/social-health-atlases>.

[20] ABS. Modelled estimates for small areas based on the 2017-18 National Health Survey. Report, Australian Bureau of Statistics, 2019.

[21] Adrijit Chakraborty, Gauri Sankar Datta, and Abhyuday Mandal. A two-component normal mixture alternative to the fay-herriot model. *arXiv preprint arXiv:1510.04482*, 2018. doi:[arXiv:1510.04482](https://arxiv.org/abs/1510.04482).

[22] Yong You and JNK Rao. Hierarchical bayes estimation of small area means using multi-level models. *Survey Methodology*, 26(2):173–181, 2000.

[23] J. N. K. Rao. Impact of frequentist and bayesian methods on survey sampling practice: A selective appraisal. *Statistical Science*, 26(2):240–256, 2011. doi:[10.1214/10-STS346](https://doi.org/10.1214/10-STS346). URL <https://doi.org/10.1214/10-STS346>.

[24] J. Hajek. Comment on "an essay on the logical foundations of survey sampling, part one". *The Foundations of Survey Sampling*, 1971.

[25] S. R. Cassy, S. Manda, F. Marques, and Mdro Martins. Accounting for sampling weights in the analysis of spatial distributions of disease using health survey data, with an application to mapping child health in malawi and mozambique. *International Journal of Environmental Research and Public Health*, 19(10), 2022. ISSN 1661-7827 (Print) 1660-4601. doi:[10.3390/ijerph19106319](https://doi.org/10.3390/ijerph19106319).

[26] Jeniffer Iriondo-Perez, Amang Sukasih, and Rachel Harter. Comparing direct survey and small area estimates of health care coverage in new york. Report, American Statistical Association, 2018.

[27] Paritosh K. Roy, Md Hasinur R. Khan, Tahmina Akter, and M. Shafiqur Rahman. Exploring socio-demographic- and geographical-variations in prevalence of diabetes and hypertension in bangladesh: Bayesian spatial analysis of national health survey data. *Spatial and Spatio-temporal Epidemiology*, 29:71–83, 2019. ISSN 1877-5845. doi:<https://doi.org/10.1016/j.sste.2019.03.003>.

[28] David A Binder. On the variances of asymptotically normal estimators from complex surveys. *International Statistical Review*, pages 279–292, 1983. ISSN 0306-7734.

[29] Peter A. Gao and Jon Wakefield. A spatial variance-smoothing area level model for small area estimation of demographic rates. *arXiv preprint arXiv:2209.02602*, 2022. doi:[arXiv:2209.02602](https://arxiv.org/abs/2209.02602).

[30] N. Best, S. Richardson, and P. Clarke. A comparison of model-based methods for small area estimation. Report, Department of Epidemiology and Public Health, Imperial College London, 2008.

[31] Andrea Riebler, Sigrunn H. Sørbye, Daniel Simpson, and Håvard Rue. An intuitive bayesian spatial model for disease mapping that accounts for scaling. *arXiv preprint arXiv:1601.01180*, 2016. doi:[arXiv:1601.01180](https://arxiv.org/abs/1601.01180).

[32] N. Tzavidis, L. C. Zhang, A. Luna, T. Schmid, and N. Rojas-Perilla. From start to finish: a framework for the production of small area official statistics. *Journal of the Royal Statistical Society*, 181(4):927–979, 2018. ISSN 0964-1998. doi:[10.1111/rssc.12364](https://doi.org/10.1111/rssc.12364). URL <https://doi.org/10.1111/rssc.12364> <Go to ISI>://WOS:000445193300002.

[33] Kirk M. Wolter. *Introduction to Variance Estimation*. Springer, New York, NY, 2007. doi:<https://doi.org/10.1007/978-0-387-35099-8>.

[34] M. Hidiroglou and Y. You. Comparison of unit level and area level small area estimators. *Survey Methodology*, 42(1):41–61, 2016.

[35] Sumonkanti Das, Jan A van den Brakel, Harm Jan Boonstra, and Stephen Haslett. *Multilevel Time Series Modelling of Antenatal Care Coverage in Bangladesh at Disaggregated Administrative Levels*. Statistics Netherlands, 2021.

[36] Stan Development Team. Stan, 2022. <https://mc-stan.org>.

[37] Tracy Qi Dong and Jon Wakefield. Modeling and presentation of vaccination coverage estimates using data from household surveys. *Vaccine*, 39(18):2584–2594, 2021. ISSN 0264-410X.

[38] Risto Lehtonen and Ari Veijanen. Logistic generalized regression estimators. *Survey Methodology*, 24(1):51–55, 1998.

[39] James Honaker and Eric Putzler. Small area estimation with multiple overimputation. *Midwest Political Science Association, Chicago*, 2011.

[40] Raydonal Ospina and Silvia L. P. Ferrari. A general class of zero-or-one inflated beta regression models. *Computational Statistics and Data Analysis*, 56(6):1609–1623, 2012. ISSN 0167-9473. doi:<https://doi.org/10.1016/j.csda.2011.10.005>. URL <https://www.sciencedirect.com/science/article/pii/S0167947311003628>.

[41] Silvia De Nicolò and Aldo Gardini. The r package tipsae: Tools for mapping proportions and indicators on the unit interval. Report, 2022.

[42] Cici Chen, Jon Wakefield, and Thomas Lumely. The use of sampling weights in bayesian hierarchical models for small area estimation. *Spatial and Spatio-temporal Epidemiology*, 11:33–43, 2014. ISSN 1877-5845. doi:<https://doi.org/10.1016/j.sste.2014.07.002>. URL <https://www.sciencedirect.com/science/article/pii/S1877584514000367>.

[43] Murray Aitkin, Charles C. Liu, and Tom Chadwick. Bayesian model comparison and model averaging for small-area estimation. *The Annals of Applied Statistics*, 3(1):199–221, 2009. URL <https://doi.org/10.1214/08-AOAS205>.

[44] Donald Malec, J. Sedransk, Christopher L. Moriarity, and Felicia B. Leclere. Small area inference for binary variables in the national health interview survey. *Journal of the American Statistical Association*, 92(439):815–826, 1997. ISSN 0162-1459. doi:[10.1080/01621459.1997.10474037](https://doi.org/10.1080/01621459.1997.10474037). URL <https://doi.org/10.1080/01621459.1997.10474037>.

[45] Andrew Gelman. Struggles with survey weighting and regression modeling. *Statistical Science*, 22(2):153–164, 2007. URL <https://doi.org/10.1214/088342306000000691>.

[46] Andrew Gelman and Thomas C Little. Poststratification into many categories using hierarchical logistic regression. *Survey Methodology*, pages 23:127–135, 1997.

[47] Matthew K. Buttice and Benjamin Highton. How does multilevel regression and poststratification perform with conventional national surveys? *Political Analysis*, 21(4):449–467, 2013. ISSN 10471987, 14764989.

[48] María Guadarrama, Domingo Morales, and Isabel Molina. Time stable empirical best predictors under a unit-level model. *Computational Statistics and Data Analysis*, 160:107226, 2021. ISSN 0167-9473. doi:<https://doi.org/10.1016/j.csda.2021.107226>.

[49] Isabel Molina and J. N. K. Rao. Small area estimation of poverty indicators. *The Canadian Journal of Statistics*, 38(3):369–385, 2010. ISSN 03195724. URL <http://www.jstor.org/stable/27896031>.

[50] Martyn Plummer. Jags: A program for analysis of bayesian graphical models using gibbs sampling. In *3rd International Workshop on Distributed Statistical Computing*, 2003.

[51] Aki Vehtari, Andrew Gelman, Daniel Simpson, Bob Carpenter, and Paul-Christian Bürkner. Rank-normalization, folding, and localization: An improved \hat{R} for assessing convergence of mcmc (with discussion). *Bayesian Analysis*, 16(2):667–718, 2021. doi:[10.1214/20-BA1221](https://doi.org/10.1214/20-BA1221). URL <https://doi.org/10.1214/20-BA1221>.

[52] Andrew Gelman, Aki Vehtari, Daniel Simpson, Charles C. Margossian, Bob Carpenter, Yuling Yao, Lauren Kennedy, Jonah Gabry, Paul-Christian Bürkner, and Martin Modrák. Bayesian workflow. *arXiv preprint arXiv:2011.01808v1*, 2020. doi:[arXiv:2011.01808v1](https://arxiv.org/abs/2011.01808).

[53] Stan Development Team. The qr reparameterization. In *Stan User’s Guide*. 2022. URL <https://mc-stan.org/docs/stan-users-guide/QR-reparameterization.html>.

[54] V. Gomez-Rubio, Nicky Best, Sylvia Richardson, Guangquan Li, and Philip Clarke. Bayesian statistics small area estimation. Report, Office for National Statistics, 2008.

[55] ABS. National Health Survey: First results methodology. Report, Australian Bureau of Statistics, 2018. URL <https://www.abs.gov.au/methodologies/national-health-survey-first-results-methodology/2017-18>.

[56] ABS. Microdata: National Health Survey [DataLab], 2017.

[57] ABS. Australian Statistical Geography Standard (ASGS), 2011. URL [https://www.abs.gov.au/websitedbs/d3310114.nsf/home/australian+statistical+geography+standard+\(asgs\)](https://www.abs.gov.au/websitedbs/d3310114.nsf/home/australian+statistical+geography+standard+(asgs)).

[58] Harvey Goldstein. *Multilevel statistical models*. John Wiley and Sons, 2011. ISBN 111995682X.

[59] A. Vehtari, A. Gelman, and J. Gabry. Practical bayesian model evaluation using leave-one-out cross-validation and waic. *Statistics and Computing*, 27(5):1413–1432, 2017. doi:[10.1007/s11222-016-9696-4](https://doi.org/10.1007/s11222-016-9696-4). URL <https://www.scopus.com/inward/record.uri?eid=2-s2.0-85026299835&doi=10.1007%2fs11222-016-9696-4&partnerID=40&md5=d4d48dc9b435386f7e4be2c5cb580f4b>.

[60] ABS. Technical paper: Socio-economic indexes for areas (SEIFA). Report, Australian Bureau of Statistics, 2016.

[61] Yair Ghitza and Andrew Gelman. Deep interactions with mrp: Election turnout and voting patterns among small electoral subgroups. *American Journal of Political Science*, 57(3):762–776, 2013. ISSN 0092-5853. doi:<https://doi.org/10.1111/ajps.12004>. URL <https://doi.org/10.1111/ajps.12004>.

[62] K. A. E. Patterson, V. Cleland, A. Venn, L. Blizzard, and S. Gall. A cross-sectional study of geographic differences in health risk factors among young australian adults: The role of socioeconomic position. *BMC Public Health*, 14(1):1–10, 2014. doi:[10.1186/1471-2458-14-1278](https://doi.org/10.1186/1471-2458-14-1278). URL <https://www.scopus.com/inward/record.uri?eid=2-s2.0-84924288776&doi=10.1186%2f1471-2458-14-1278&partnerID=40&md5=775e49b9ba2c4478ae77d0e0c641ce77>.

[63] Hee Cheol Chung and Gauri Sankar Datta. Bayesian hierarchical spatial models for small area estimation. Report, Center for Statistical Research and Methodology, 2020.

[64] Connor Donegan, Yongwan Chun, and Daniel A. Griffith. Modeling community health with areal data: Bayesian inference with survey standard errors and spatial structure. *International Journal of Environmental Research and Public Health*, 18(13):6856, 2021. ISSN 1660-4601. URL <https://www.mdpi.com/1660-4601/18/13/6856>.

[65] W. R. Bell, G. S. Datta, and M. Ghosh. Benchmarking small area estimators. *Biometrika*, 100(1):189–202, 2013. ISSN 0006-3444. doi:[10.1093/biomet/ass063](https://doi.org/10.1093/biomet/ass063). URL <https://doi.org/10.1093/biomet/ass063>://WOS:000315623900011.

[66] J. L. Zhang and J. Bryant. Fully bayesian benchmarking of small area estimation models. *Journal of Official Statistics*, 36(1):197–223, 2020. ISSN 0282-423X. doi:[10.2478/jos-2020-0010](https://doi.org/10.2478/jos-2020-0010). URL <https://doi.org/10.2478/jos-2020-0010>://WOS:000520863200010.

[67] Earl W. Duncan, Susanna M. Cramb, Joanne F. Aitken, Kerrie L. Mengersen, and Peter D. Baade. Development of the australian cancer atlas: spatial modelling, visualisation, and reporting of estimates. *International Journal of Health Geographics*, 18(1):21, 2019. ISSN 1476-072X. doi:[10.1186/s12942-019-0185-9](https://doi.org/10.1186/s12942-019-0185-9). URL <https://doi.org/10.1186/s12942-019-0185-9>.

[68] Sylvia Richardson, Andrew Thomson, Nicky Best, and Paul Elliott. Interpreting posterior relative risk estimates in disease-mapping studies. *Environmental Health Perspectives*, 112(9):1016–1025, 2004. ISSN 0091-6765 1552-9924. doi:[10.1289/ehp.6740](https://doi.org/10.1289/ehp.6740).

[69] Pierre E Jacob, Lawrence M Murray, Chris C Holmes, and Christian P Robert. Better together? statistical learning in models made of modules. *arXiv preprint arXiv:1708.08719*, 2017. doi:[arXiv:1708.08719](https://doi.org/10.4236/ojs.201708719).

[70] Glenn Shafer and Vladimir Vovk. A tutorial on conformal prediction. *Journal of Machine Learning Research*, 9(3), 2008. ISSN 1532-4435.

[71] Elizabeth Bersson and Peter D Hoff. Optimal conformal prediction for small areas. *arXiv preprint arXiv:2204.08122*, 2022.

SUPPLEMENTAL MATERIALS FOR “A TWO-STAGE BAYESIAN SMALL AREA ESTIMATION METHOD FOR PROPORTIONS”

James Hogg¹ Jessica Cameron^{2,4} Susanna Cramb³ Peter Baade^{1,4} Kerrie Mengerson^{1,2}

¹Centre for Data Science, Queensland University of Technology

²School of Mathematical Sciences, Queensland University of Technology

³Australian Centre for Health Services Innovation, School of Public Health and Social Work, Queensland University of Technology

⁴Descriptive Epidemiology, Cancer Council Queensland

A Proposed method: further details

A.1 Definition for S1 sampling variance

Here we show that the sampling variance for a S1 estimate are lower bounded by the direct estimate sampling variance. Initially let,

$$\frac{\sum_{j \in r_i} w_{ij} y_{ij}}{n_i} = \frac{\sum_{j \in r_i} w_{ij} y_{ij}}{n_i} + \frac{\sum_{j \in r_i} w_{ij} p_{ij}}{n_i} - \frac{\sum_{j \in r_i} w_{ij} p_{ij}}{n_i},$$

which can be rewritten as,

$$\hat{\mu}_i^{S1} = \hat{\mu}_i^D + \hat{B}_i,$$

where

$$\hat{B}_i = \frac{\sum_{j \in r_i} w_{ij} (p_{ij} - y_{ij})}{n_i},$$

is the difference between $\hat{\mu}_i^{S1}$ and $\hat{\mu}_i^D$. Thus, by treating both y_{ij} and w_{ij} as fixed quantities and by definition assuming $\text{cov}(\hat{\mu}_i^D, \hat{B}_i) = 0$, the sampling variance of the S1 estimator is given by,

$$\hat{v}(\hat{\mu}_i^{S1}) \leq \hat{v}(\hat{\mu}_i^D) + \hat{v}(\hat{B}_i),$$

where the \leq is used as simple empirical results show that without assuming y_{ij} as fixed the $\text{cov}(\hat{\mu}_i^D, \hat{B}_i) < 0$.

The specification for $\hat{v}(\hat{\mu}_i^{S1})$ ensures that poorly specified logistic models will give large sampling variances, because $\hat{v}(\hat{B}_i)$ will be large. Furthermore, as p_{ij} tends to y_{ij} , $\hat{v}(\hat{\mu}_i^{S1}) \approx \hat{v}(\hat{\mu}_i^D)$.

A.2 Inference methods for the TSLN model

As mentioned in Section 2.2, we fit the TSLN model in two stages. The steps are threefold:

1. Fit the individual level logistic model, and collect all T posterior draws of $\hat{\theta}_i^{S1}$ and γ_i^{S1} .

2. Calculate the posterior mean of γ_i^{S1} , defined as $\bar{\gamma}_i^{S1}$, and the posterior variance of $\hat{\theta}_i^{S1}$, denoted $\hat{v}(\hat{\theta}_i^{S1})$.
3. Take a random sample of posterior draws for each $\hat{\theta}_i^{S1}$, to create a matrix of draws $\hat{\theta}_i^{S1,its} \in \mathbb{R}^{\tilde{T} \times m}$, where $\tilde{T} < T$ is the number of posterior draws randomly sampled. In this work, we set $\tilde{T} = \frac{T}{2}$.

By letting $\hat{\theta}_i^{S1,its} = (\hat{\theta}_{i1}^{S1,its}, \dots, \hat{\theta}_{i\tilde{T}}^{S1,its})$ be the vector of randomly selected posterior draws for area i , the TSLN-S2 model is specified as,

$$\hat{\theta}_i^{S1,its} \sim N(\hat{\theta}_i, \hat{v}(\hat{\theta}_i^{S1}))^{1/\tilde{T}} \quad i = 1, \dots, m \quad \text{Eq. A.2.1}$$

$$\hat{\theta}_i \sim N(\hat{\theta}_i, \bar{\gamma}_i^{S1}) \quad i = 1, \dots, m, \quad \text{Eq. A.2.2}$$

where $\hat{\theta}_i$ follows (11) in Section 2.1.4. To ensure that the uncertainty of the parameters of the TSLN-S2 model are not mediated by the arbitrary choice of \tilde{T} , we scale the likelihood contributions by $1/\tilde{T}$. This approach follows similar intuition to pseudo-likelihood [? ?].

The specification above can be viewed as a type of FH model where the variance of the sampling model is an independent combination of sampling and model variance. Thus, Eq. A.2.1 and Eq. A.2.2 can be collapsed into $\hat{\theta}_i^{S1,its} \sim N(\hat{\theta}_i, \bar{\gamma}_i^{S1} + \hat{v}(\hat{\theta}_i^{S1}))$.

There are simpler and also more complex approaches to estimating the parameters of the TSLN model. The approach of Das et al. [?] and Gao and Wakefield [?] was to treat the posterior means for $\hat{\theta}_i^{S1}$ and γ_i^{S1} from the stage 1 model as known quantities in the stage 2 model. However, this approach neglects the uncertainty in the first-stage logistic model. In a more complex model setup, we would also add $\gamma_i^{S1,its} \sim N(\bar{\gamma}_i^{S1}, \hat{v}(\gamma_i^{S1}))$, rather than treating $\bar{\gamma}_i^{S1}$ as a fixed quantity.

Further extensions could incorporate the correlation structure between posterior draws for $\hat{\theta}_i^{S1}$ and γ_i^{S1} . One could initially treat the diagonal elements of the variance-covariance matrices, $\sum \in \mathbb{R}^{m \times m}$, as fixed, but estimate a constant correlation between all areas (i.e. use an exchangeable correlation structure). A further step would be to consider an unstructured correlation matrix, by using the empirical variance-covariance matrices, $\widetilde{\sum} \in \mathbb{R}^{m \times m}$, and a multivariate normal distribution. In this case, $\hat{\theta}_i^{S1,its} \sim \text{MVN}(\hat{\theta}, \widetilde{\sum})$, where $\hat{\theta} = (\hat{\theta}_1, \dots, \hat{\theta}_m)$. Note that Das et al. [?] found that incorporating the covariances between area predictions did little to improve the bias or variance of their final estimates. In our simulation study, we found little correlation between the posterior draws for different areas.

B Existing methods: further details

B.1 Seminal model-based methods

Fay-Herriot (FH) model Let $\hat{\theta}_i^D$ and γ_i^D be the known (and fixed) area level direct estimates and sampling variances for areas $i = 1, \dots, m$ and $\mathbf{Z} \in \mathbb{R}^{M \times (q^a+1)}$ be the area level design matrix with corresponding regression coefficients, $\boldsymbol{\lambda} \in \mathbb{R}^{(q^a+1) \times 1}$, for the q^a area level covariates. A fully Bayesian FH model is given by,

$$\hat{\theta}_i^D \sim N(\theta_i, \gamma_i^D) \quad i = 1, \dots, m \quad \text{Eq. B.1.1}$$

$$\theta_i = \mathbf{Z}_i \boldsymbol{\lambda} + v_i \quad i = 1, \dots, M \quad \text{Eq. B.1.2}$$

$$v_i \sim N(0, \sigma_v^2) \quad i = 1, \dots, M$$

where independent priors are used for the other model parameters ($\boldsymbol{\lambda}, \sigma_v$). The small area estimate for area i is given by the marginal posterior of $\hat{\theta}_i$. By construction, the FH model gives $\hat{\theta}_i$, the synthetic estimate in Eq. B.1.2, when γ_i^D is very large, but $\hat{\theta}_i^D$ when γ_i^D is very small.

Nested error (NER) model With access to detailed individual level continuous outcome data, δ_{ij} , individual level models become another avenue for SAE [?]. The Bayesian nested error (NER) model is [?],

$$\begin{aligned} \delta_{ij} &\sim N(\mathbf{x}_{ij} \boldsymbol{\beta} + e_i, \sigma_e^2) \quad j = 1, \dots, n_i; i = 1, \dots, m \\ e_i &\sim N(0, \sigma_e^2) \quad i = 1, \dots, M. \end{aligned} \quad \text{Eq. B.1.3}$$

Independent priors are used for the model parameters. By assuming that N_i is large [?], the empirical best linear unbiased predictor (EBLUP) is calculated as,

$$\hat{\theta}_i = \bar{\mathbf{X}}_i \boldsymbol{\beta} + e_i, \quad i = 1, \dots, M$$

where we distinguish between the design matrix, $\mathbf{x} \in \mathbb{R}^{n \times (q^u+1)}$, for the q^u individual level covariates and the area level means for the same covariates, $\bar{\mathbf{X}} \in \mathbb{R}^{M \times (q^u+1)}$.

Unlike the Bayesian FH model (Eq. B.1.1), the NER Eq. B.1.3, does not incorporate the individual level sampling weights and is thus not design unbiased [?]. Although individual level models have been shown to outperform area level models [?], the core limitation of Eq. B.1.3 is that one must have access to the individual level and known population means for all q^u covariates; restricting one to census covariates only.

B.2 Area level models for proportions

Normal-logit model A simple adaption of the FH model (Eq. B.1.1) for proportions is achieved by accommodating the bounds of the direct proportion estimates in the link function. Liu, Lahiri, and Kalton [?] describes this approach via a normal-logit model.

$$\begin{aligned} \hat{\mu}_i^D &\sim N(\mu_i, \psi_i^D) \quad i = 1, \dots, M \\ \text{logit}(\mu_i) &= \mathbf{Z}_i \boldsymbol{\lambda} + v_i \quad i = 1, \dots, M \\ v_i &\sim N(0, \sigma_v^2) \quad i = 1, \dots, M \end{aligned} \quad \text{Eq. B.2.1}$$

Liu, Lahiri, and Kalton [?] argue that Eq. B.2.1 is applicable only when n_i is sufficiently large, resulting in small sample variances, ψ_i^D and thus approximate normality of $\hat{\mu}_i^D$.

Binomial model An alternative approach to the normal logit model is to model the area level sample counts, $\hat{Y}_i = \sum_{j \in s_i} y_{ij}$, with a binomial distribution [? ? ?], $\hat{Y}_i \sim \text{Binomial}(n_i, \mu_i)$, where the linear predictor and random effects are the same as those in Eq. B.2.1.

Although the binomial model does not automatically accommodate the sample design, interested readers are referred to Vandendijck *et al.* [?] and Chen, Wakefield, and Lumely [?] for binomial models that do. These authors adjust both

\widehat{Y}_i and n_i according to the sample design to derive the effective number of counts \tilde{Y}_i and effective sample size, \tilde{n}_i . In practice, their method results in non-integer values for \tilde{Y}_i and \tilde{n}_i , which requires generalizing the discrete binomial distribution when fitting Bayesian models in probabilistic programming languages such as Stan.

Beta model The Beta distribution, which is naturally bounded between 0 and 1, is a favourable choice for modelling small area proportions [? ? ?]. Although formally parameterized by two parameters, $\kappa^{(1)}$ and $\kappa^{(2)}$ say, that control the shape and scale, it is common to adopt the following mean-precision parameterization [?] where $\kappa^{(1)} = \phi\mu$ and $\kappa^{(2)} = \phi - \phi\mu = \phi - \kappa^{(1)}$. The parameter $\mu \in (0, 1)$ is the mean of the bounded outcome, whilst $\phi > 0$ can be interpreted as a precision parameter. Hence for $Z \in (0, 1)$, note that

$$\begin{aligned} E[Z] &= \frac{\kappa^{(1)}}{\kappa^{(1)} + \kappa^{(2)}} = \mu \\ \text{Var}[Z] &= \frac{\kappa^{(1)}\kappa^{(2)}}{(\kappa^{(1)} + \kappa^{(2)})^2(\kappa^{(1)} + \kappa^{(2)} + 1)} = \frac{\mu(1 - \mu)}{\phi + 1}. \end{aligned}$$

Following the specification of the FH model [?], ϕ is considered known and is calculated as

$$\frac{\mu_i(1 - \mu_i)}{\psi_i^D} - 1. \quad \text{Eq. B.2.2}$$

The Bayesian area level FH Beta model follows directly,

$$\begin{aligned} \hat{\mu}_i^D &\sim \text{Beta}\left(\kappa_i^{(1)} = \mu_i\phi_i, \kappa_i^{(2)} = \phi_i - \kappa_i^{(1)}\right) \quad i = 1, \dots, m \\ \text{logit}(\mu_i) &= \mathbf{X}_i\boldsymbol{\beta} + v_i \quad i = 1, \dots, M \\ v_i &\sim N(0, \sigma_v^2) \quad i = 1, \dots, M, \end{aligned} \quad \text{Eq. B.2.3}$$

where the proportion estimate for area i is given by μ_i .

Unlike other implementations of FH Beta models [? ?], we specify the shape parameters in terms of ϕ_i directly rather than pre-calculating the effective sample size, $\tilde{n}_i = \phi_i + 1$. Below we show how these implementations are equivalent.

$$\begin{aligned} \hat{v}_{\text{srs}}(\hat{\mu}_i^D) &= \frac{\hat{\mu}_i^D(1 - \hat{\mu}_i^D)}{n_i} \\ \text{deff}_i &= \frac{\psi_i^D}{\hat{v}_{\text{srs}}(\hat{\mu}_i^D)} \\ \phi_i + 1 &= \frac{n_i}{\text{deff}_i}, \\ \phi_i + 1 &= \frac{\left(\frac{n_i}{1}\right)}{\left(\frac{\psi_i^D}{\left(\frac{\hat{\mu}_i^D(1 - \hat{\mu}_i^D)}{n_i}\right)}\right)} = \frac{n_i \left(\frac{\hat{\mu}_i^D(1 - \hat{\mu}_i^D)}{n_i}\right)}{\psi_i^D} \\ \phi_i &= \frac{\hat{\mu}_i^D(1 - \hat{\mu}_i^D)}{\psi_i^D} - 1 \end{aligned}$$

Unfortunately, the FH Beta model has several statistical and computational limitations, some of which are summarized in Table 1. The first is a constraint on the mean of the Beta distribution. In order to ensure that the shape parameters remain strictly positive,

$$\hat{\mu}_i \in \left(\frac{1 - \sqrt{1 - 4\psi_i^D}}{2}, \frac{1 + \sqrt{1 - 4\psi_i^D}}{2}\right). \quad \text{Eq. B.2.4}$$

Very imprecise or unstable direct estimates can give biased posterior distributions for $\hat{\mu}_i$ since its range tends to 0 as ψ_i^D tends to 0.25.

As a result of the first limitation, the bounds on $\hat{\mu}_i$ must be applied to all M areas to ensure consistency between estimates for both sampled and nonsampled areas. One requires a version of the GVF in (12) that can impute sampling variances for all M — even those areas with no data. Arguably it makes little sense to estimate sampling variances for areas with no sample data, even if this is only for computational reasons. In this work, we assume that $n_i \propto N_i$, and then use $\log(N_i)$ as the single covariate in \mathbf{L} . We also set $f(x) = \log\left(\frac{x}{0.25+x}\right)$, which respects the constraint $\psi_i^D \leq 0.25$ imposed by the Beta distribution. In practice, covariate choice for a GVF (of the form in (12)) for use in a FH Beta model, is restricted to covariates available for all areas, which makes it impossible to accommodate sample sizes and direct estimates, which are expected *a priori* to be very predictive of the sampling variances.

A computational limitation of the Beta model is its possible bimodal behaviour; a disastrous affair for standard MCMC methods. A constraint $\kappa^{(1)}, \kappa^{(2)} > 1$ must be imposed to ensure the Beta distribution remains unimodal. However, in the case of the FH Beta model, this constraint places a very restrictive upper limit on the values of ψ_i^D . Any areas with large sampling variances generally produce bimodal Beta distributions and thus cannot be accommodated into the FH Beta model. To improve convergence, we constrain $\hat{\mu}_i \in (0.03, 0.97)$. This is a valid computational constraint and is unlikely to affect model performance.

A final limitation is that the FH Beta model is particularly affected by instability of direct estimates because the likelihood for the Beta distribution becomes undefined if $\hat{\mu}_i^D$ is exactly equal to 0 or 1.

Empirical logistic-normal model By targeting the boundary issues with the normal-logit model (Eq. B.2.1), Mercer *et al.* [?] and then Cassy *et al.* [?] used an empirical logit transformation of the direct estimates.

$$\begin{aligned} \text{logit}(\hat{\mu}_i^D) &\sim N(\theta_i, \gamma_i^D) \quad i = 1, \dots, m \\ \gamma_i^D &= \psi_i^D [\hat{\mu}_i^D (1 - \hat{\mu}_i^D)]^{-2} \quad i = 1, \dots, m \\ \theta_i &= \text{logit}(\mu_i) = \mathbf{Z}_i \boldsymbol{\lambda} + v_i \quad i = 1, \dots, M \\ v_i &\sim N(0, \sigma_v^2) \quad i = 1, \dots, M \end{aligned} \quad \text{Eq. B.2.5}$$

The small area estimate for area i is given by $\mu_i = \text{logit}^{-1}(\theta_i)$.

B.3 Individual level models for proportions

Pseudo-likelihood logistic mixed model To extend the NER model to the binary setting and accommodate the sample design, one can use an individual level Bayesian pseudo-likelihood logistic mixed model [? ?].

$$\begin{aligned} y_{ij} &\sim \text{Bernoulli}(p_{ij})^{\tilde{w}_{ij}} \quad j = 1, \dots, n_i, i = 1, \dots, m \\ \text{logit}(p_{ij}) &= \mathbf{x}_{ij} \boldsymbol{\beta} + e_i \quad j = 1, \dots, N_i, i = 1, \dots, M \end{aligned} \quad \text{Eq. B.3.1}$$

Because of the nonlinear link function, the area level proportion estimate is derived by aggregating across the observed and unobserved individuals in each small area,

$$\hat{\mu}_i = \frac{1}{N_i} \left(\sum_{j \in r_i} y_{ij} + \sum_{j \in r_i^C} \hat{p}_{ij} \right), \quad \text{Eq. B.3.2}$$

where \hat{p}_{ij} is estimated using the posterior distributions of the model parameters, $\boldsymbol{\beta}, \sigma_e$, for $j \in r_i^C$.

The motivation for Bayesian pseudo-likelihood is to ensure that the posterior distribution is similar (at least asymptotically) with that from the same specified model fit to the entire population [?]. For an arbitrary outcome vector \mathbf{y} , sampling weights, \mathbf{w} and model parameters $\boldsymbol{\theta}$, the posterior distribution is specified as

$$p(\boldsymbol{\theta} | \mathbf{y}) \propto \left[\prod_{i=1}^N p(y_i | \boldsymbol{\theta})^{w_i} \right] p(\boldsymbol{\theta}),$$

where $\prod_{i=1}^N p(y_i|\boldsymbol{\theta})^{w_i}$ denotes the pseudo likelihood for the sample.

C Simulation study: further details

C.1 Algorithm

Below we give more details on the simulation study described in Section 4. We generated a census using steps 1-4 below, and then drew $D = 100$ unique samples (repetitions) from this census using step 5.

Step 1 Create a M -length vector of area level proportions, \mathbf{U} , with values equally spaced between P^L and P^U (e.g. $\mathbf{U} = (U_1 = 0.1, \dots, U_M = 0.4)$). Sample a random vector of area specific population sizes, $\mathbf{N} = (N_1, \dots, N_M)$ from the set $\{500, 3000\}$. Note that $N = \sum_{i=1}^M N_i$. Next, using a binomial distribution sample the area counts, $Y_i \sim \text{Binomial}(n = N_i, p = U_i)$. Finally, *uncount* Y_i to create the binary outcome $y_{ij} \in \{0, 1\}$ for individual j in area i . For example, in area 1 the vector $\mathbf{y}_1 = (y_{11}, \dots, y_{1N_1})$, will be composed of Y_1 1's and $N_1 - Y_1$ 0's.

Step 2 To simulate individual level covariates (one survey-only categorical covariate, \mathbf{x}^s with three groups, and one continuous covariate, \mathbf{x}^{cs} available in both the census and survey), first sample two standard normal vectors of length N , denoted $\mathbf{e}^s, \mathbf{e}^{cs}$. Then calculate the following two continuous covariates, $x_{*,ij}^s = y_{ij} + \alpha^s e_{ij}^s$ and $x_{*,ij}^{cs} = y_{ij} + \alpha^{cs} e_{ij}^{cs}$, where α^s and α^{cs} control the predictive power of the individual level covariates. Small values of α^s and α^{cs} will provide greater correlation between the outcome and the individual level covariates. Finally, convert \mathbf{x}_*^s into a categorical covariate, \mathbf{x}^s , using appropriate quantiles and standardize \mathbf{x}_*^{cs} to create \mathbf{x}^{cs} .

Step 3 To generate an area level covariate first calculate the true area level proportions, $\mu_i = \frac{1}{N_i} \sum_{j=1}^{N_i} y_{ij}$. Note that μ is constant for all 100 repetitions. Following a similar method to Step 2, simulate a random standard normal vector of length M , denoted \mathbf{g} , and calculate a continuous covariate, $k_{*,i}^a = \text{logit}(\mu_i) + ug_i$, where u controls the predictive power of the area level covariate (similar to α^s and α^{cs} above). As before, we standardize \mathbf{k}_*^a to create \mathbf{k}^a , and then expand this vector and include it in the census dataset. The simulated census (of size $N \times 5$) has columns $\mathbf{y}, \mathbf{x}^s, \mathbf{x}^{cs}, \mathbf{k}^a, \mathbf{I}$, where $\mathbf{I} \in \{1, \dots, M\}$ is an integer vector that defines the area for each individual.

Step 4 We fix the sampling fraction at 0.4% and $m = 60$, and then calculate the fixed area sample sizes, $n_i = \text{round}(\frac{100}{60} \times 0.004 \times N_i)$. Next, by following the simulation method used by Hidiroglou and You [?], we simulate $z_{ij} = \mathbb{I}(y_{ij} = 0) + 0.8h_{ij}$ for all individuals, where h_{ij} is a random draw from an exponential distribution with rate equal to 1. The values of z_{ij} are used to determine each individual's sampling probability, $\pi_{ij} = z_{ij} \left(\sum_{j=1}^{N_i} z_{ij} \right)^{-1}$, and sampling weight, $w_{ij} = n_i^{-1} \pi_{ij}^{-1}$, based on the fixed area sample size. The calculation of π_{ij} makes individuals with $y_{ij} = 0$ more likely to be sampled (i.e. the sampled design is informative).

Step 5 Select 60 out of the 100 areas proportional to their size (i.e. randomly select areas according to $\frac{N_i}{N}$). Within each selected area, draw an informative sample of size n_i based on the sampling probabilities, π_{ij} . Finally, rescale the sampling weights to ensure that the sum within area i equals N_i .

The simulation algorithm was purposely stochastic and thus complete control via the various simulation parameters was not definite. This is particularly true for the covariate effect sizes. We conducted an extensive grid search across simulation parameter values (using crude but fast frequentist methods) to determine the values that gave reasonable model coefficients. In this work, we found that $\alpha^{cs} = 1$ gave reasonable coefficients. Although N_i and n_i were fixed, the areas to be sampled and which individuals were sampled in each selected area was stochastic, resulting in different n for each repetition d . Note that u , which has an inverse affect on the predictive power of the area level covariate, was set to 0.05 for Sc1-Sc2 and 0.01 for Sc3-Sc6 to ensure \mathbf{k}^a , the area level covariate, was sufficiently predictive.

C.2 Summary

The fourth column in Table 3 is derived as follows. For each repetition, we calculate the median of the per-area ratio of the S1 and direct sampling variances using

$$100 \left(\left(\frac{\bar{\gamma}_{id}^{S1} + \tilde{v}(\hat{\theta}_{id}^{S1})}{\gamma_{id}^D} \right) - 1 \right),$$

which is expected to be greater than 0 as $\bar{\gamma}_{id}^{S1} > \gamma_{id}^D$.

The fifth column is derived as follows. For each repetition we derive the ratio of the MAB,

$$\begin{aligned}\text{MAB}_d^D &= \frac{1}{M} \sum_i |\hat{\mu}_{id}^D - \mu_i| \\ \text{MAB}_d^{\text{S1}} &= \frac{1}{M} \sum_i |\bar{\hat{\mu}}_{id}^{\text{S1}} - \mu_i| \\ \text{Ratio}_d &= 100 \left(1 - \frac{\text{MAB}_d^{\text{S1}}}{\text{MAB}_d^D} \right)\end{aligned}$$

for the direct and S1 estimates, where $\bar{\hat{\mu}}_{id}^{\text{S1}}$ is the posterior median of $\hat{\mu}_{id}^{\text{S1}}$. In Table 3 we give the median of Ratio_d across the 100 repetitions.

C.3 Other performance metrics

Let $\bar{\hat{\mu}}_{id}$ denote the posterior median of a model's parameter of interest for area i for repeat d [?]. The following frequentist metrics were used in work by Chen, Wakefield, and Lumely [?], and are summarized in [Table 1](#).

$$\begin{aligned}\text{Bias} &= \frac{1}{M} \sum_{i=1}^M \left(\bar{\hat{\mu}}_i - \mu_i \right), \text{ where } \bar{\hat{\mu}}_i = \frac{1}{D} \sum_{d=1}^D \bar{\hat{\mu}}_{id} \\ \text{Variance} &= \frac{1}{M} \sum_{i=1}^M \left(\frac{1}{D-1} \sum_{d=1}^D \left(\bar{\hat{\mu}}_{id} - \bar{\hat{\mu}}_i \right)^2 \right) \\ \text{MSE} &= (\text{Bias})^2 + \text{Variance} \end{aligned} \tag{Eq. C.3.1}$$

		Sampled areas		Nonsampled areas	
		MSE		MSE	
50-50	Sc1	D	4.73 (12.78)	0.82 (2.22)	
		BETA	2.05 (5.54)	3.55 (9.59)	
		BIN	3.55 (9.59)	0.78 (2.11)	
		ELN	1.87 (5.05)	0.31 (0.84)	
		LOG	0.90 (2.43)		
		TSLN	0.37 (1.00)	0.37 (1.00)	
	Sc2	D	4.62 (12.16)	0.83 (2.18)	
		BETA	1.99 (5.24)	3.54 (9.32)	
		BIN	3.54 (9.32)	0.83 (2.18)	
		ELN	1.85 (4.87)	0.31 (0.82)	
		LOG	0.88 (2.32)		
		TSLN	0.38 (1.00)	0.38 (1.00)	
Rare	Sc3	D	3.77 (10.77)	0.94 (2.69)	
		BETA	1.09 (3.11)	1.48 (4.23)	
		BIN	1.49 (4.26)	2.03 (5.80)	
		ELN	2.84 (8.11)	0.43 (1.23)	
		LOG	1.08 (3.09)		
		TSLN	0.35 (1.00)	0.35 (1.00)	
	Sc4	D	3.77 (10.19)	0.94 (2.47)	
		BETA	1.09 (2.95)	1.48 (3.89)	
		BIN	1.49 (4.03)	2.03 (5.34)	
		ELN	2.84 (7.68)	0.43 (1.13)	
		LOG	1.08 (2.92)		
		TSLN	0.37 (1.00)	0.38 (1.00)	
Common	Sc5	D	3.06 (14.57)	0.19 (0.86)	
		BETA	0.78 (3.71)	3.00 (13.64)	
		BIN	3.00 (14.29)	0.24 (1.09)	
		ELN	0.51 (2.43)	0.17 (0.77)	
		LOG	0.34 (1.62)		
		TSLN	0.21 (1.00)	0.22 (1.00)	
	Sc6	D	3.31 (17.42)	0.16 (0.84)	
		BETA	0.92 (4.84)	2.99 (15.74)	
		BIN	2.99 (15.74)	0.23 (1.21)	
		ELN	0.63 (3.32)	0.17 (0.89)	
		LOG	0.35 (1.84)		
		TSLN	0.19 (1.00)	0.19 (1.00)	

Table 1: Frequentist MSE ($\times 10^{-2}$) (Eq. C.3.1). D denotes the Hajek [?] direct estimator given in (1). Bold numbers represent the lowest MSE value in each column and scenario for sampled and nonsampled areas. Gray numbers in brackets give the ratio of the value to that of the TSLN model.

		Individual level				Area level	
		$x^s(2)$	$x^s(3)$	x^{cs}	σ_e	k^a	σ_v
50-50	Sc1	BETA				0.36	0.60
		BIN				0.35	0.14
		ELN				0.44	0.74
		LOG		1.20	0.65	0.41	
		TSLN-S1	1.49	3.07	1.22	0.72	0.39
		TSLN-S2				0.38	0.12
Rare	Sc2	BETA				0.37	0.58
		BIN				0.34	0.14
		ELN				0.46	0.74
		LOG		1.20	0.64	0.42	
		TSLN-S1	0.74	1.57	1.20	0.65	0.41
		TSLN-S2				0.40	0.11
Common	Sc3	BETA				0.47	0.65
		BIN				0.49	0.21
		ELN				0.96	2.10
		LOG		1.22	0.93	0.57	
		TSLN-S1	1.35	3.17	1.27	0.97	0.59
		TSLN-S2				0.60	0.17
	Sc4	BETA				0.47	0.65
		BIN				0.49	0.21
		ELN				0.96	2.10
		LOG		1.22	0.93	0.57	
		TSLN-S1	0.75	1.59	1.25	0.97	0.59
		TSLN-S2				0.61	0.17
	Sc5	BETA				0.56	0.55
		BIN				0.52	0.14
		ELN				0.58	0.39
		LOG		1.17	0.46	0.53	
		TSLN-S1	1.65	3.01	1.19	0.55	0.55
		TSLN-S2				0.52	0.11
	Sc6	BETA				0.57	0.58
		BIN				0.51	0.14
		ELN				0.60	0.42
		LOG		1.15	0.50	0.54	
		TSLN-S1	0.79	1.49	1.17	0.51	0.53
		TSLN-S2				0.55	0.10

Table 2: Median of posterior medians of model parameters across all $D = 100$ repetitions by model and scenario. Given the scale of the data is different depending on the model, coefficients cannot be easily compared. The first group of x^s is the reference group. $x^s(2)$ refers to the regression coefficient for the indicator for the second group of x^s . By construction the coefficients for levels 2 and 3 of x^s are larger for Sc1, Sc3 and Sc5.

D Application: further details

D.1 Covariates

TSLN-S1 The breadth of individual level covariates available in the NHS is enormous. We found an initial set of candidate covariates using pseudo-likelihood and `1me4` [?]. As mentioned in Section 2.1.2, we preferred models with a lower *SR* and a *ALC* closer to 1.

On top of those covariates included in the LOG model (sex, age, and marital status), we used a variety of others, listed below. Note that we square root transformed, denoted as `sqrt`, some of the continuous covariates to reduce their skew.

- Individual level categorical covariates with the number of categories given in brackets. For details see [Table 3](#).
 - High school (6)
 - Kessler psychological distress score (5)
 - Qualifications (9)
 - Self-assessed health (5)
 - laborforce status (6)
 - Number of daily smokers in the household (3)
 - Tenure type of household (5)
 - Whether indigenous members in household (3)
- Area level
 - Categorical
 - * Index of Relative Socio-Economic Disadvantage (IRSD) from the Socio-Economic Indexes for Areas (SEIFA) by the ABS (ABS 2016): 10 decile groups of increasing socio-economic disadvantage (SA2s in group 1 are classified as the most disadvantaged)
 - * State: 4 groups
 - Continuous
 - * Occupation: proportion of SA2 who are professionals
 - * Indigenous status (`sqrt`): proportion of SA2 who identify as Aboriginal and/or Torres Strait Islander
 - * Income: proportion of SA2 with a high weekly personal income (specifically between AUD\$1,500 and AUD\$1,750)
 - * Unemployment rate (`sqrt`): proportion of persons in labor force in SA2 who are unemployed
 - * Household composition: proportion of households in SA2 with four people

	Categories
Age	15-19 20-24 25-34 35-44 45-54 55-64 65-74 75-84 85+
Sex	Males Females
Registered marital status	Never married Widowed Divorced Separated Married
Qualifications	Postgraduate Degree Graduate Diploma/Graduate Certificate Bachelor Degree Advanced Diploma/Diploma Certificate III/IV

	Certificate I/II Certificate not further defined No non-school qualification Level not determined
laborforce status	Employed, working full-time Employed, working part-time Unemployed, looking for full-time work Unemployed, looking for part-time work Unemployed, looking for full-time or part-time work Not in the labor force
High school	Year 12 or equivalent Year 11 or equivalent Year 10 or equivalent Year 9 or equivalent Year 8 or below Never attended school
Kessler psychological distress score	Low/moderate level of psychological distress (5-11) High/very high level of psychological distress (12-25) No applicable No asked Unable to determine
Tenure type of household	Owner without a mortgage Owner with a mortgage Renter Other Not stated
Self-assessed health	Excellent Very good Good Fair Poor
Number of daily smokers in the household	Less than 2 More than 1 Not stated
Whether indigenous members in household	Non-indigenous only household Indigenous only household Mixed household

Table 3: Categories for the individual level covariates used in the TSLN and LOG models for current smoking prevalence. Most of the categories for these covariates were derived by the Australian Bureau of Statistics. For details of the definitions, we refer the reader to publicly available data dictionaries. An exception is the Number of daily smokers in the household variable, which was collapsed from its original form to ensure the variable did not *perfectly* predict current smokers.

We also found a significant improvement in model fit by adding a hierarchical prior on a risk factor categorical covariate constructed from every unique combination of sex and age and the following binary risk factors: insufficient physical activity, insufficient fruit and vegetable consumption, overweight, and risky alcohol consumption. All the binary risk factors were defined according to current Australian health guidelines with definitions given in [Table 4](#).

TSLN-S2 Deriving variable selection metrics for the TSLN-S2 requires additional thought; the input data are vectors of posterior draws, making the definition of the “data” difficult to determine. To align with previous work where the uncertainty inherent in fitting the first stage model is not considered, we use an approximation to the LOOCV. The `loo` package requires log-likelihood, $\mathbb{L}(\cdot)$ evaluations for all data points and posterior draws [?]. Below we restate Eq. A.2.1 and Eq. A.2.2 as a reminder,

$$\begin{aligned}\hat{\theta}_i^{\text{S1,its}} &\sim N\left(\hat{\hat{\theta}}_i, \hat{v}\left(\hat{\theta}_i^{\text{S1}}\right)\right) & i = 1, \dots, m \\ \hat{\hat{\theta}}_i &\sim N\left(\theta_i, \hat{\gamma}_i^{\text{S1}}\right) & i = 1, \dots, m.\end{aligned}$$

	Definition	Notes
Overweight	By using the common cut-offs [? ? ?], those with a BMI greater or equal to 25 are coded as 1.	This includes those who are obese.
Alcohol	Those who did not meet the revised 2020 Australian National Health and Medical Research Council (NHMRC) guidelines [?] are coded as 1.	The guidelines stipulate that adults should drink no more than 10 standard drinks a week and no more than 4 standard drinks on any one day.
Physical activity	Those who did not meet the 2014 Australian Department of Health Physical Activity guidelines [?] were coded as 1.	The NHMRC guidelines, which closely mirror those given by the WHO [?], stipulate that each week adults should either do 2.5 to 5 hours of moderate-intensity physical activity or 1.25 to 2.5 hours of vigorous-intensity physical activity or an equivalence combination of both. In addition, the guidelines recommend muscle-strengthening activities at least 2 days each week. This binary variable was based on both their leisure and workplace physical activity levels.
Diet	Those who did not meet the fruit and vegetable 2013 NHMRC Australian Dietary guidelines [?] were coded as 1.	The NHMRC guidelines stipulate two servings of fruit and five servings of vegetables per day.

Table 4: Definitions for the binary variables used in the risk factor categorical covariate. The categorical covariate has every unique combination of the four binary variables in this table and age and sex.

We take the expectation of $\hat{\theta}_i$ and treat it as data. In this way, we use

$$\mathbb{L} \left(\theta_{it}; \mathbb{E} \left(\hat{\theta}_i \right), \bar{\gamma}_i^{S1} \right) \quad i = 1, \dots, M; t = 1, \dots, T,$$

to derive the LOOCV using the `loo` package. Although this approach to deriving the LOOCV ignores the uncertainty in fitting the first stage model, it aligns with previous two-stage approaches [? ?].

The 2016 Australian census collects a large amount of demographic data which can be used as SA2-level covariates in our models. For a single demographic factor, such as qualification, there are several categories, resulting in numerous proportion variables for qualification alone (bachelor degree, postgraduate degree, etc). Instead of relying on a set of single proportion covariates and risk missing important predictors, we used Principal Components analysis on 84 SA2-level census covariates. We found that the first six principal components had 63% of the variation and when used as covariates provided superior fit than models using the actual census proportions. Thus, the following eight SA2-level variables were included as fixed effects in the TSLN-S2 and ELN models; IRSD, state and principal components one to six.

D.2 Spatial prior

The BYM2 prior proposed by Riebler *et al.* [?] is a linear combination of an intrinsic CAR prior [?] and an unstructured normal prior. It places a single variance parameter, σ_δ^2 , on the combined components with the help of a mixing parameter, $\rho \in (0, 1)$, that represents the amount of spatially structured as opposed to unstructured residual variation. The BYM2 prior is

$$\begin{aligned} \delta_i &= \sigma_\delta \left(s_i \sqrt{\rho/\kappa} + v_i \sqrt{1-\rho} \right) & i = 1, \dots, M \\ s_i &\sim N \left(\frac{\sum_{k=1}^M W_{ik} s_k}{\sum_{k=1}^M W_{ik}}, \frac{1}{\sum_{k=1}^M W_{ik}} \right) & i = 1, \dots, M \\ v_i &\sim N(0, 1) & i = 1, \dots, M, \end{aligned} \quad \text{Eq. D.2.1}$$

where $\mathbf{W} \in \mathbb{R}^{M \times M}$ is the spatial weight matrix, which defines the neighborhood structure of the SA2s. As is common in disease mapping [?], we use the binary contiguous specification where $W_{ik} = 1$ if area i and area k are neighbors

and zero otherwise. The parameter κ is a known scaling factor, while ρ is generally estimated from the data [?]. Following the recommendations by Gomez-Rubio *et al.* [?], Mohadjer *et al.* [?] and Banerjee, Carlin, and Gelfand [?], the ICAR prior for $\mathbf{s} = (s_1, \dots, s_M)$ is declared for all areas and thus the s_i 's for non-sampled areas are implicitly imputed during MCMC. Following advice by Gomez-Rubio *et al.* [?], we also tried fitting an unstructured, ICAR and BYM2 prior at a higher administrative level; specifically the statistical areas level 3 (SA3s) which are constructed from aggregated SA2s. However, we found no discernible improvement in model fit.

D.3 Benchmarking

Let $\widehat{C}_{k[i]}^D$ and $\widehat{v}(\widehat{C}_{k[i]}^D)$ be the direct Hajek [?] estimate and sampling variance for state $k = 1, \dots, 4$ (see (1) and (2) in Section 1.1). The values of $\widehat{C}_{k[i]}^D$ will be the benchmark values, with the goal that our population-weighted model-based estimate of this quantity

$$\widetilde{C}_{k[i]} = \frac{\sum_{i \in S_k} \hat{\mu}_i N_i}{\sum_{i \in S_k} N_i} \quad k = 1, \dots, 4 \quad \text{Eq. D.3.1}$$

agrees at least approximately with $\widehat{C}_{k[i]}^D$, where $\hat{\mu}_i$ is the modeled prevalence estimate for SA2 i . Note that S_k is the subset of integers that determines which SA2s are contained within state k (i.e. $\mathbb{I}(i \in S_k) = 1$ if SA2 i is in state k and zero otherwise). Inexact fully benchmarking takes the form,

$$\widetilde{C}_{k[i]} \sim N\left(\widehat{C}_{k[i]}^D, \left(\epsilon \times \sqrt{\widehat{v}(\widehat{C}_{k[i]}^D)}\right)^2\right) \quad k = 1, \dots, 4, \quad \text{Eq. D.3.2}$$

where $0 < \epsilon < 1$ is a discrepancy measure. Setting $\epsilon = 0$ gives exact benchmarking, whilst $\epsilon = 1$ enables the model to accommodate the benchmarks in line with their respective accuracy. We enforced stronger concordance between $\widetilde{C}_{k[i]}$ and $\widehat{C}_{k[i]}^D$ by fixing $\epsilon = 0.3$. With our SA4 level direct estimates, $\epsilon = 0.3$ gives standard deviations in Eq. D.3.2 that range from 0.002 to 0.003.

Given that SA2-level estimates from the LOG model are derived via poststratification (e.g. a post-model calculation), we cannot use Bayesian benchmarking. Instead, we use an exact ratio-adjusted estimator to benchmark the LOG model estimates [?]. We first derived an adjustment factor, $R_{k[i]t}^B$, for the k th state and t th posterior draw,

$$\begin{aligned} \widetilde{Y}_{k[i]t} &= \sum_{i \in S_k} \hat{\mu}_{it} N_i \\ \widehat{Y}_{k[i]} &= \widehat{C}_{k[i]}^D N_k \\ R_{k[i]t}^B &= \frac{\widetilde{Y}_{k[i]t}}{\widehat{Y}_{k[i]}}, \end{aligned}$$

where $\widetilde{Y}_{k[i]t}$ and $\widehat{Y}_{k[i]}$ are the modeled and direct estimates of the smoking counts in state k , respectively. Note that N_k is the population in state k . Then the benchmarked LOG model estimates are calculated as,

$$\hat{\mu}_{it}^B = \frac{\hat{\mu}_{it}}{R_{k[i]t}^B}. \quad \text{Eq. D.3.3}$$

which, by design, ensures that $\sum_{i=1}^M \mathbb{I}(i \in S_k) \hat{\mu}_{it}^B N_i / N_k = \widehat{C}_{k[i]}^D$ for all posterior draws. Finally, posterior summaries are applied to $\hat{\mu}_i^B$. Note that Zhang and Bryant [?] found that exact benchmarking provided larger reductions in posterior variance than that of inexact Bayesian benchmarking.

D.4 Comparative performance

To compare models, we derived modeled and direct estimates at a higher administrative level: statistical areas level 4 (SA4). There are 65 SA4's across the east coast of Australia, with a median sample and population size of 148 and 220,000, respectively.

The motivation for comparing the models at the SA4 rather than SA2 level, is that we can plausibly treat the SA4 level direct estimates as the *truth*; approximately 75% of the direct estimates have coefficients of variation below 25%. Note that although the SA4-level estimates are far more precise and stable than those at the SA2 level, we acknowledge the limitations inherent in treating these as the truth. Thus, these performance results are illustrative at best, but presented here for completeness.

The SA4 level modeled and direct estimates are calculated using population-weighted averages of the model-based SA2-level estimates and (1), respectively. We compare the models using RRMSE, ARB, and coverage (see Section 4.0.1). In addition, given that the SA4-level estimates also have uncertainty, we quantify the overlap of the direct and modeled intervals. Overlap probabilities give the proportion of the modeled interval that is contained within the direct estimate interval. A high probability is preferred and a value of 1 denotes that the modeled interval is entirely within the direct estimate interval. To summarize the overlap probabilities across the 65 SA4s, we take a weighted mean where the weights are the inverse direct estimate standard deviations.

[Fig. 1](#) displays equivalence plots and [Table 5](#) compares the mean RRMSE and ARB across all SA4s and summarises the credible interval sizes, coverage and overlap probabilities for the three models.

Similar to the findings in the simulation study, [Table 5](#) shows that the TSLN model provides smaller MRRMSE and credible interval sizes at the SA4 level. Although the TSLN provides poor Bayesian coverage and higher MARB, our model is preferable in terms of overlap.

D.5 Further plots for case study

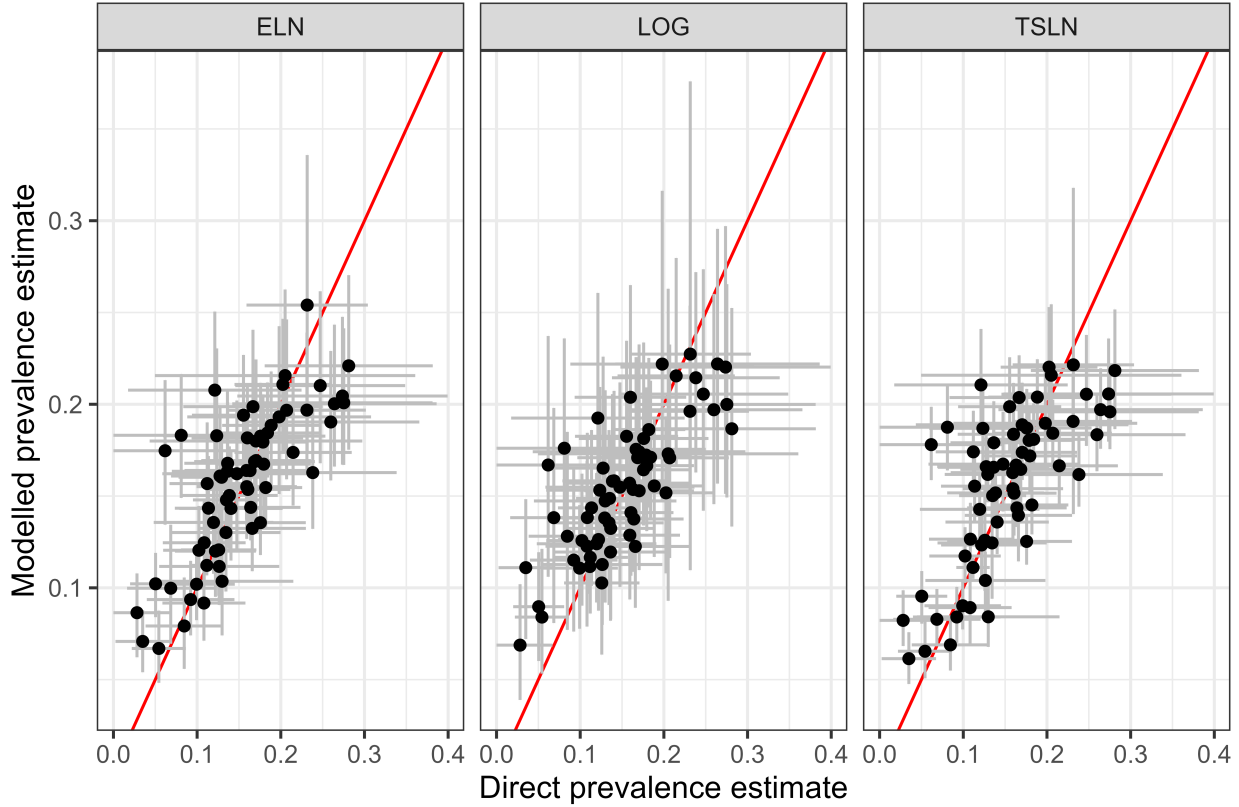


Figure 1: Comparison of the modeled and direct prevalence estimates at the SA4 level. Along with the point estimates, the plot gives the 95% intervals represented as gray lines. The diagonal red line represents equivalence between the modeled and direct estimates.

		MRRMSE	MARB	CI width	Coverage	Overlap
Benchmarked	ELN	0.29	0.24	0.06	0.68	0.78
	LOG	0.35	0.27	0.09	0.83	0.73
	TSLN	0.29	0.26	0.04	0.48	0.80
Not benchmarked	ELN	0.35	0.30	0.07	0.66	0.72
	LOG	0.55	0.28	0.22	0.98	0.52
	TSLN	0.29	0.25	0.05	0.55	0.75

Table 5: Performance metrics for the three models when predicting SA4-level prevalence estimates. The table provides MRRMSE, MARB, median width of 95% posterior credible interval (CI width), coverage and the weighted mean of overlap probabilities. Results are given separately when benchmarking is and is not used.

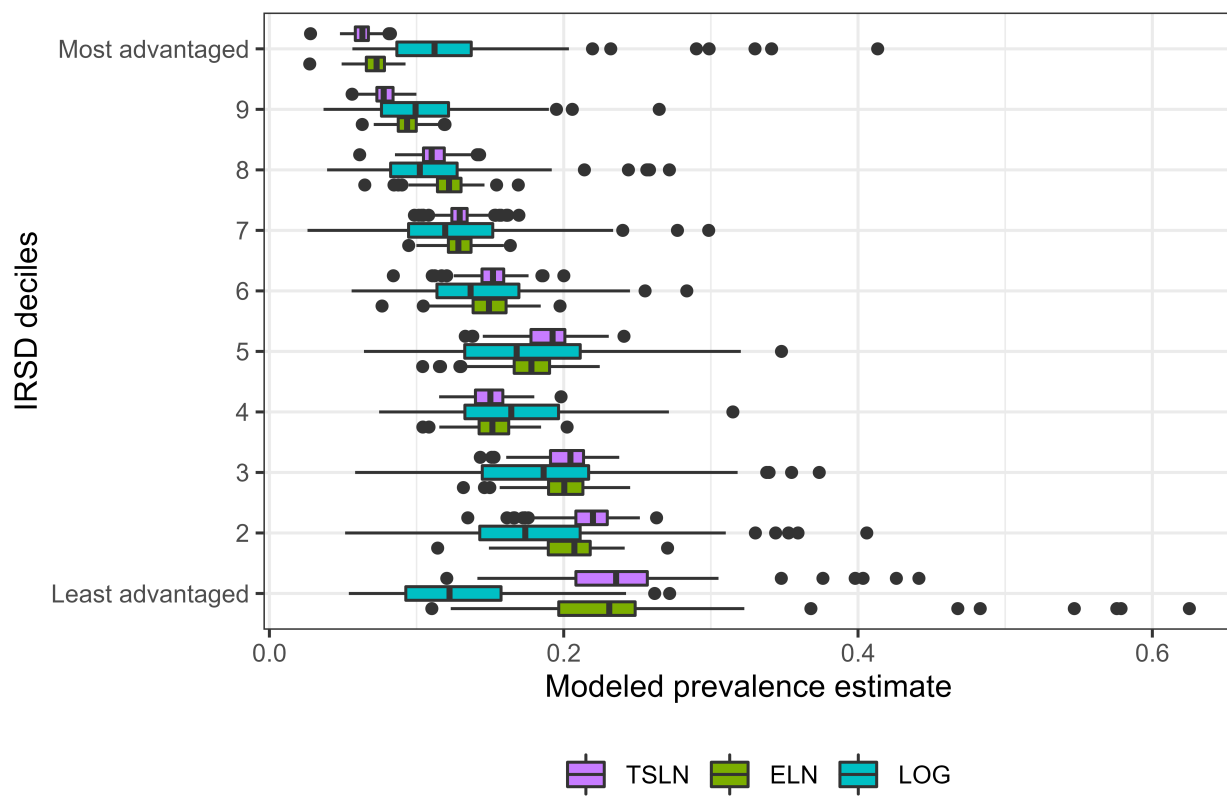


Figure 2: Comparison of the modeled SA2 level current smoking prevalence estimates by IRSD categories. Each boxplot summarises the posterior medians of the prevalence for a specific IRSD deciles and model.

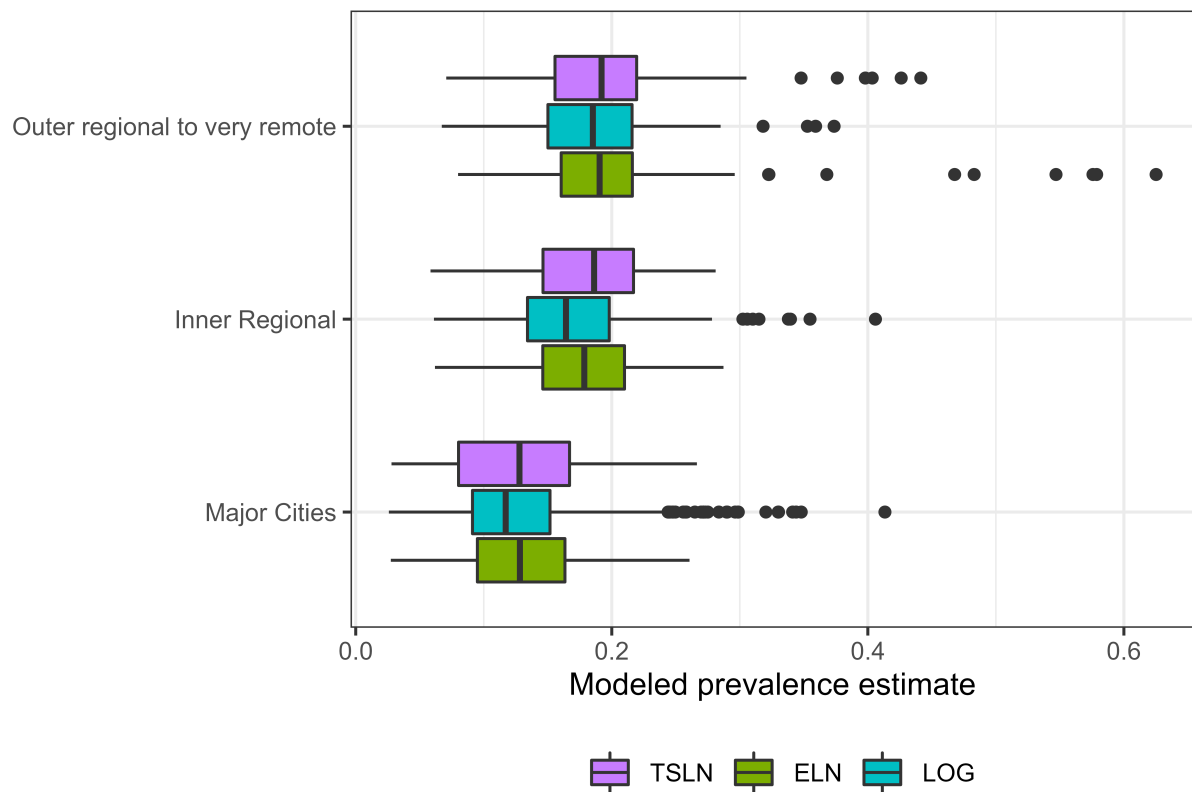


Figure 3: Comparison of the modeled SA2 level current smoking prevalence estimates by remoteness.

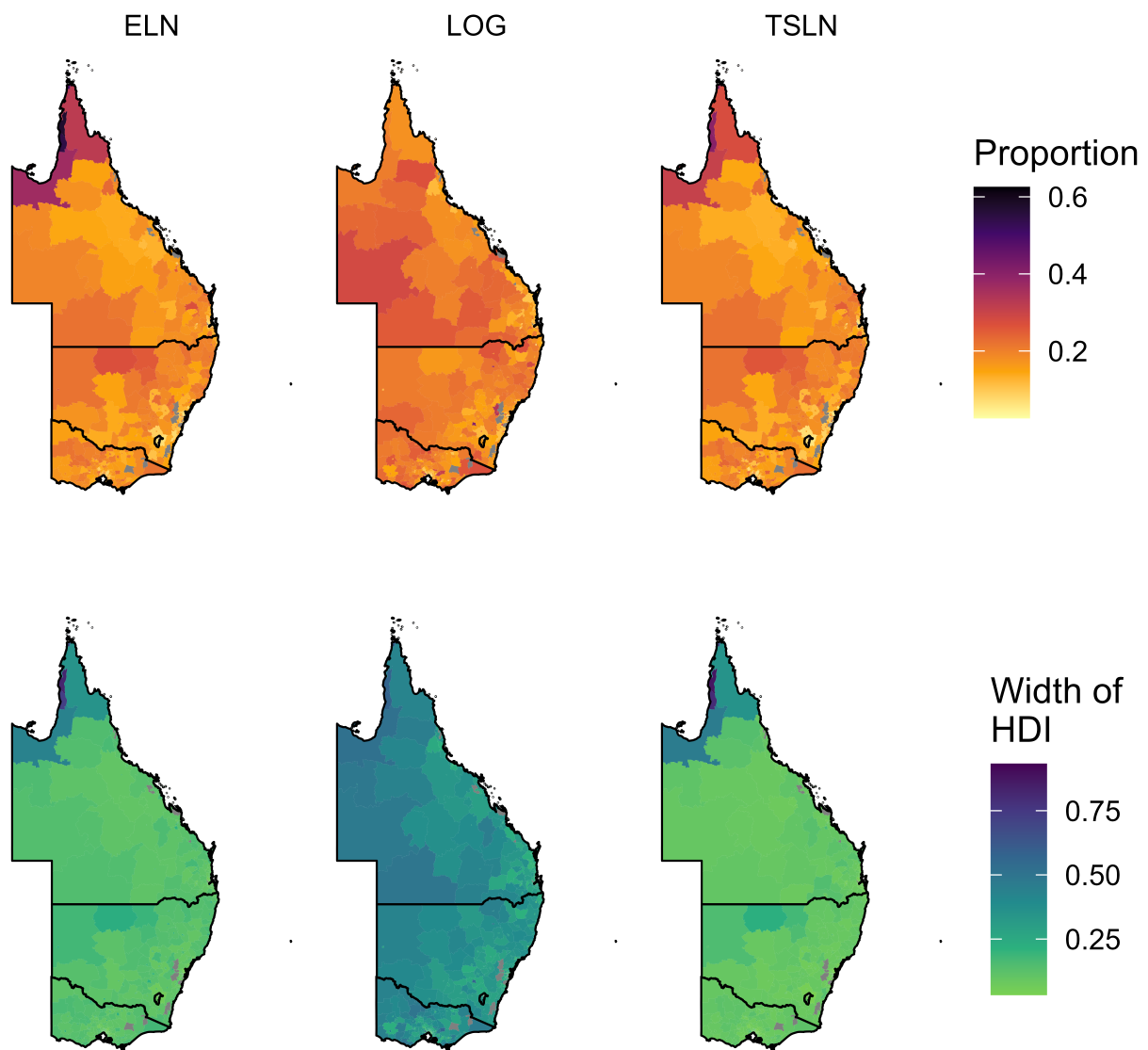


Figure 4: Choropleth maps displaying the modeled estimates of current smoking prevalence for 1630 SA2s on the east coast of Australia. For each model, we mapped the posterior medians and width of the 95% HDI. Note that some values are lower than the range of color scales shown — for these values, the lowest color is used.

Sydney

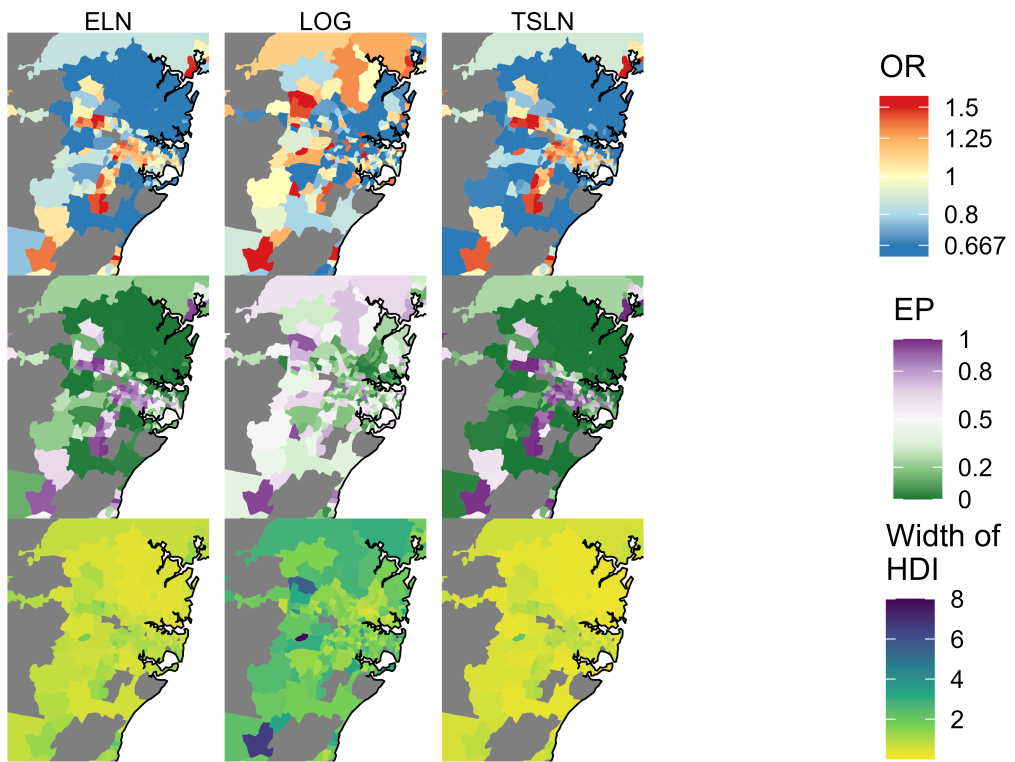


Figure 5: Choropleth maps displaying the modeled ORs for smoking prevalence in 282 SA2s in and around Sydney, Australia. For each model, we mapped the posterior medians, exceedance probabilities (EPs) and the width of the 95% HDI. Note that some values are lower than the range of color scales shown — for these values, the lowest color is used. Gray areas were excluded from estimation due to having 2016-2017 EPs smaller or equal to 10.